

# The Cosmic Microwave Background

Arthur Kosowsky

*Department of Physics and Astronomy, Rutgers University, Piscataway, NJ 08854-8019*

`kosowsky@physics.rutgers.edu`

## ABSTRACT

This set of lectures provides an overview of the basic theory and phenomenology of the cosmic microwave background. Topics include a brief historical review; the physics of temperature and polarization fluctuations; acoustic oscillations of the primordial plasma; the space of inflationary cosmological models; current and potential constraints on these models from the microwave background; and constraints on inflation. These lectures were given at the Italian Society of Gravitational Physics Summer School “Relativistic Cosmology: Theory and Observation” in Como, Italy (May 2000).

## 1. Introduction

It is widely accepted that the field of cosmology is entering an era dubbed “precision cosmology.” Data directly relevant to the properties and evolution of the universe is flooding in by the terabyte (or soon will be). Such vast quantities of data were the purview only of high energy physics just a few years ago; now expertise from this area is being coopted by some astromers to help deal with our wealth of information. In the past decade, cosmology has gone from a data-starved science in which often highly speculative theories went unconstrained to a data-driven pursuit where many models have been ruled out and the remaining “standard cosmology” will be tested with stringent precision.

The cosmic microwave background radiation is at the center of this revolution. The radiation present today as a 2.7 K thermal background originated when the universe was denser by a factor of  $10^9$  and younger by a factor of around  $5 \times 10^4$ . The radiation provides the most distant direct image of the universe we can hope to see, at least until gravitational radiation becomes a useful astronomical data source. The microwave background radiation is extremely uniform, varying in temperature by only a few parts in  $10^5$  over the sky (apart from an overall dipole variation arising from our peculiar motion through the microwave background’s rest frame); its departure from a perfect blackbody spectrum has yet to be detected.

The very existence of the microwave background provides crucial support for the Hot Big Bang cosmological model: the universe began in a very hot, dense state from which it expanded and cooled. The microwave background visible today was once in thermal equilibrium with the primordial plasma of the universe, and the universe at that time was highly uniform. Crucially, the universe could not have been perfectly uniform at that time or no structures would have formed subsequently. The study of small temperature and polarization fluctuations in the microwave background, reflecting small variations in density and velocity in the early universe, have the potential to provide the most precise constraints on the overall properties of the universe of any data source. The reasons are that (1) the universe was very simple at the time imaged by the microwave background and is extremely well-described by linear perturbation theory around a completely homogeneous and isotropic cosmological spacetime; and (2) the physical processes relevant at that time are all simple and very well understood. The microwave background is essentially unique among astrophysical systems in these regards.

The goal behind these lectures is to provide a qualitative description of the physics of the microwave background, an appreciation for the microwave background’s cosmological importance, and an understanding of what kinds of constraints may be placed on cosmological models. These lectures are not intended to be a definitive technical reference to the microwave background. Unfortunately, such a reference does not really exist at this time, but I have attempted to provide pedagogically useful references to other literature. I have also not attempted to give a complete bibliography; please do not consider this article to give definitive references to any topics mentioned. A recent review of the microwave background with a focus on potential particle physics constraints is Kamionkowski and Kosowsky (1999). A more general review of the microwave background and large-scale structure with references to many early microwave background articles is White *et al.* (1994).

## 2. A Brief Historical Perspective

The story of the serendipitous discovery of the microwave background in 1965 is widely known, so I will only briefly summarize it here. A recent book by the historian of science Helge Kraugh (1996) is a careful and authoritative reference on the history of cosmology, from which much of the information in this section was obtained. Arno Penzias and Robert Wilson, two radio astronomers at Bell Labs in Crawford, New Jersey, were using a sensitive microwave horn radiometer originally intended for talking to the early Telstar telecommunications satellites. When Bell Labs decided to get out of the communications satellite business in 1963, Penzias and Wilson began to use the radiometer to measure radio emission from the

Cassiopeia A supernova remnant. They detected a uniform noise source, which was assumed to come from the apparatus. But after many months of checking the antenna and the electronics (including removal of a bird’s nest from the horn), they gradually concluded that the signal might actually be coming from the sky. When they heard about a talk given by P.J.E. Peebles of Princeton predicting a 10 K blackbody cosmological background, they got in touch with the group at Princeton and realized they had detected the cosmological radiation. At the time, Peebles was collaborating with Dicke, Roll, and Wilkinson in a concerted effort to detect the microwave background. The Princeton group wound up confirming the Bell Labs discovery a few months later. Penzias and Wilson published their result in a brief paper with the unassuming title of “A measurement of excess antenna temperature at  $\lambda = 7.3$  cm” (Penzias and Wilson 1965); a companion paper by the Princeton group explained the cosmological significance of the measurement (Dicke et al 1965). The microwave background detection was a stunning success of the Hot Big Bang model, which to that point had been well outside the mainstream of theoretical physics. The following years saw an explosion of work related to the Big Bang model of the expanding universe. To the best of my knowledge, the Penzias and Wilson paper was the second-shortest ever to garner a Nobel Prize, awarded in 1978. (Watson and Crick’s renowned double helix paper wins by a few lines.)

Less well known is the history of earlier probable detections of the microwave background which were not recognized as such. Tolman’s classic monograph on thermodynamics in an expanding universe was written in 1934, but a blackbody relic of the early universe was not predicted theoretically until 1948 by Alpher and Herman, a by-product of their pioneering work on nucleosynthesis in the early universe. Prior to this, Andrew McKellar (1940) had observed the population of excited rotational states of CN molecules in interstellar absorption lines, concluding that it was consistent with being in thermal equilibrium with a temperature of around 2.3 Kelvin. Walter Adams also made similar measurements (1941). Its significance was unappreciated and the result essentially forgotten, possibly because World War II had begun to divert much of the world’s physics talent towards military problems.

Alpher and Herman’s prediction of a 5 Kelvin background contained no suggestion of its detectability with available technology and had little impact. Over the next decade, George Gamow and collaborators, including Alpher and Herman, made a variety of estimates of the background temperature which fluctuated between 3 and 50 Kelvin (e.g. Gamow 1956). This lack of a definitive temperature might have contributed to an impression that the prediction was less certain than it actually was, because it aroused little interest among experimenters even though microwave technology had been highly developed through radar work during the war. At the same time, the incipient field of radio astronomy was getting started. In 1955, Emile Le Roux undertook an all-sky survey at a wavelength of  $\lambda = 33$  cm, finding an isotropic emission corresponding to a blackbody temperature of  $T = 3 \pm 2$  K (Denisse

*et al.* 1957). This was almost certainly a detection of the microwave background, but its significance was unrealized. Two years later, T.A. Shmaonov observed a signal at  $\lambda = 3.2$  cm corresponding to a blackbody temperature of  $4 \pm 3$  K independent of direction (see Sharov and Novikov 1993, p. 148). The significance of this measurement was not realized, amazingly, until 1983! (Kragh 1996). Finally in the early 1960’s the pieces began to fall in place: Doroshkevich and Novikov (1964) emphasized the detectability of a microwave blackbody as a basic test of Gamow’s Hot Big Bang model. Simultaneously, Dicke and collaborators began searching for the radiation, prompted by Dicke’s investigations of the physical consequences of the Brans-Dicke theory of gravitation. They were soon scooped by Penzias and Wilson’s discovery.

As soon as the microwave background was discovered, theorists quickly realized that fluctuations in its temperature would have fundamental significance as a reflection of the initial perturbations which grew into galaxies and clusters. Initial estimates of the amplitude of temperature fluctuations were a part in a hundred; this level of sensitivity was attained by experimenters after a few years with no observed fluctuations. Thus began a quarter-century chase after temperature anisotropies in which the theorists continually revised their estimates of the fluctuation amplitude downwards, staying one step ahead of the experimenters’ increasingly stringent upper limits. Once the temperature fluctuations were shown to be less than a part in a thousand, baryonic density fluctuations did not have time to evolve freely into the nonlinear structures visible today, so theorists invoked a gravitationally dominant dark matter component (structure formation remains one of the strongest arguments in favor of non-baryonic dark matter). By the end of the 1980’s, limits on temperature fluctuations were well below a part in  $10^4$  and theorists scrambled to reconcile standard cosmology with this small level of primordial fluctuations. Ideas like late-time phase transitions at redshifts less than  $z = 1000$  were taken seriously as a possible way to evade the microwave background limits (see, e.g., Jaffe *et al.* 1990). Finally, the COBE satellite detected fluctuations at the level of a few parts in  $10^5$  (Smoot *et al.* 1990), just consistent with structure formation in inflation-motivated Cold Dark Matter cosmological models. The COBE results were soon confirmed by numerous ground-based and balloon measurements, sparking the intense theoretical and experimental interest in the microwave background over the past decade.

### 3. Physics of Temperature Fluctuations

The minute temperature fluctuations present in the microwave background contain a wealth of information about the fundamental properties of the universe. In order to understand the reasons for this and the kinds of information available, an appreciation of the

underlying physical processes generating temperature and polarization fluctuations is required. This section and the following one give a general description of all basic physics processes involved in producing microwave background fluctuations.

First, one practical matter. Throughout these lectures, common cosmological units will be employed in which  $\hbar = c = k_b = 1$ . All dimensionful quantities can then be expressed as powers of an energy scale, commonly taken as GeV. In particular, length and time both have units of  $[\text{GeV}]^{-1}$ , while Newton's constant  $G$  has units of  $[\text{GeV}]^{-2}$  since it is defined as equal to the square of the inverse Planck mass. These units are very convenient for cosmology, because many problems deal with widely varying scales simultaneously. For example, any computation of relic particle abundances (e.g. primordial nucleosynthesis) involves both a quantum mechanical scale (the interaction cross-section) and a cosmological scale (the time scale for the expansion of the universe). Conversion between these cosmological units and physical (cgs) units can be achieved by inserting needed factors of  $\hbar$ ,  $c$ , and  $k_b$ . The standard textbook by Kolb and Turner (1990) contains an extremely useful appendix on units.

### 3.1. Causes of temperature fluctuations

Blackbody radiation in a perfectly homogeneous and isotropic universe, which is always adopted as a zeroth-order approximation, must be at a uniform temperature, by assumption. When perturbations are introduced, three elementary physical processes can produce a shift in the apparent blackbody temperature of the radiation emitted from a particular point in space. All temperature fluctuations in the microwave background are due to one of the following three effects.

The first is simply a change in the intrinsic temperature of the radiation at a given point in space. This will occur if the radiation density increases via adiabatic compression, just as with the behavior of an ideal gas. The fractional temperature perturbation in the radiation just equals the fractional density perturbation.

The second is equally simple: a doppler shift if the radiation at a particular point is moving with respect to the observer. Any density perturbations within the horizon scale will necessarily be accompanied by velocity perturbations. The induced temperature perturbation in the radiation equals the peculiar velocity (in units of  $c$ , of course), with motion towards the observer corresponding to a positive temperature perturbation.

The third is a bit more subtle: a difference in gravitational potential between a particular point in space and an observer will result in a temperature shift of the radiation propagating between the point and the observer due to gravitational redshifting. This is

known as the Sachs-Wolfe effect, after the original paper describing it (Sachs and Wolfe, 1967). This paper contains a completely straightforward general relativistic calculation of the effect, but the details are lengthy and complicated. A far simpler and more intuitive derivation has been given by Hu and White (1997) making use of gauge transformations. The Sachs-Wolfe effect is often broken into two pieces, the usual effect and the so-called Integrated Sachs-Wolfe effect. The latter arises when gravitational potentials are evolving with time: radiation propagates into a potential well, gaining energy and blueshifting in the process. As it climbs out, it loses energy and redshifts, but if the depth of the potential well has increased during the time the radiation propagates through it, the redshift on exiting will be larger than the blueshift on entering, and the radiation will gain a net redshift, appearing cooler than it started out. Gravitational potentials remain constant in time in a matter-dominated universe, so to the extent the universe is matter dominated during the time the microwave background radiation freely propagates, the Integrated Sachs-Wolfe effect is zero. In models with significantly less than critical density in matter (i.e. the currently popular  $\Lambda$ CDM models), the redshift of matter-radiation equality occurs late enough that the gravitational potentials are still evolving significantly when the microwave background radiation decouples, leading to a non-negligible Integrated Sachs-Wolfe effect. The same situation also occurs at late times in these models; gravitational potentials begin to evolve again as the universe makes a transition from matter domination to either vacuum energy domination or a significantly curved background spatial metric, giving an additional Integrated Sachs-Wolfe contribution.

### 3.2. A formal description

The early universe at the epoch when the microwave background radiation begins propagating freely, around a redshift of  $z = 1100$ , is a conceptually simple place. Its constituents are “baryons” (including protons, helium nuclei, and electrons, even though electrons are not baryons), neutrinos, photons, and dark matter particles. The neutrinos and dark matter can be treated as interacting only gravitationally since their weak interaction cross-sections are too small at this energy scale to be dynamically or thermodynamically relevant. The photons and baryons interact electromagnetically, primarily via Compton scattering of the radiation from the electrons. The typical interaction energies are low enough for the scattering to be well-approximated by the simple Thomson cross section. All other scattering processes (e.g. Thomson scattering from protons, Rayleigh scattering of radiation from neutral hydrogen) have small enough cross-sections to be insignificant, so we have four species of matter with only one relevant (and simple) interaction process among them. The universe is also very close to being homogeneous and isotropic, with small perturbations in density and velocity

on the order of a part in  $10^5$ . The tiny size of the perturbations guarantees that linear perturbation theory around a homogeneous and isotropic background universe will be an excellent approximation.

Conceptually, the formal description of the universe at this epoch is quite simple. The unperturbed background cosmology is described by the Friedmann-Robertson-Walker (FRW) metric, and the evolution of the cosmological scale factor  $a(t)$  in this metric is given by the Friedmann equation (see the lectures by Peacock in this volume). The evolution of the free electron density  $n_e$  is determined by the detailed atomic physics describing the recombination of neutral hydrogen and helium; see Seager *et al.* (2000) for a detailed discussion. At a temperature of around 0.5 eV, the electrons combine with the protons and helium nuclei to make neutral atoms. As a result, the photons cease Thomson scattering and propagate freely to us. The microwave background is essentially an image of the “surface of last scattering”. Recombination must be calculated quite precisely because the temperature and thickness of this surface depend sensitively on the ionization history through the recombination process.

The evolution of first-order perturbations in the various energy density components and the metric are described with the following sets of equations:

- The photons and neutrinos are described by distribution functions  $f(\mathbf{x}, \mathbf{p}, t)$ . A fundamental simplifying assumption is that the energy dependence of both is given by the blackbody distribution. The space dependence is generally Fourier transformed, so the distribution functions can be written as  $\Theta(\mathbf{k}, \hat{\mathbf{n}}, t)$ , where the function has been normalized to the temperature of the blackbody distribution and  $\hat{\mathbf{n}}$  represents the direction in which the radiation propagates. The time evolution of each is given by the Boltzmann equation. For neutrinos, collisions are unimportant so the Boltzmann collision term on the right side is zero; for photons, Thomson scattering off electrons must be included.
- The dark matter and baryons are in principle described by Boltzmann equations as well, but a fluid description incorporating only the lowest two velocity moments of the distribution functions is adequate. Thus each is described by the Euler and continuity equations for their densities and velocities. The baryon Euler equation must include the coupling to photons via Thomson scattering.
- Metric perturbation evolution and the connection of the metric perturbations to the matter perturbations are both contained in the Einstein equations. This is where the subtleties arise. A general metric perturbation has 10 degrees of freedom, but four of these are unphysical gauge modes. The physical perturbations include two degrees of freedom constructed from scalar functions, two from a vector, and two remaining tensor perturbations (Mukhanov *et al.* 1992). Physically, the scalar perturbations correspond

to gravitational potential and anisotropic stress perturbations; the vector perturbations correspond to vorticity and shear perturbations; and the tensor perturbations are two polarizations of gravitational radiation. Tensor and vector perturbations do not couple to matter evolving only under gravitation; in the absence of a “stiff source” of stress energy, like cosmic defects or magnetic fields, the tensor and vector perturbations decouple from the linear perturbations in the matter.

A variety of different variable choices and methods for eliminating the gauge freedom have been developed. The subject can be fairly complicated. A detailed discussion and comparison between the Newtonian and synchronous gauges, along with a complete set of equations, can be found in Ma and Bertschinger (1995); also see Hu *et al.* (1998). An elegant and physically appealing formalism based on an entirely covariant and gauge-invariant description of all physical quantities has been developed for the microwave background by Challinor and Lasenby (1999) and Gebbie *et al.* (2000), based on earlier work by Ehlers (1993) and Ellis and Bruni (1989). A more conventional gauge-invariant approach was originated by Bardeen (1980) and developed by Kodama and Sasaki (1984).

The Boltzmann equations are partial differential equations, which can be converted to hierarchies of ordinary differential equations by expanding their directional dependence in Legendre polynomials. The result is a large set of coupled, first-order linear ordinary differential equations which form a well-posed initial value problem. Initial conditions must be specified. Generally they are taken to be so-called adiabatic perturbations: initial curvature perturbations with equal fractional perturbations in each matter species. Such perturbations arise naturally from the simplest inflationary scenarios. Alternatively, isocurvature perturbations can also be considered: these initial conditions have fractional density perturbations in two or more matter species whose total spatial curvature perturbation cancels. The issue of numerically determining initial conditions is discussed below in Sec. 5.2.

The set of equations are numerically stiff before last scattering, since they contain the two widely discrepant time scales: the Thomson scattering time for electrons and photons, and the (much longer) Hubble time. Initial conditions must be set with high accuracy and an appropriate stiff integrator must be employed. A variety of numerical techniques have been developed for evolving the equations. Particularly important is the line-of-sight algorithm first developed by Seljak and Zaldarriaga (1996) and then implemented by them in the publicly-available CMBFAST code (see <http://www.sns.ias.edu/~matiasz/CMBFAST/cmbfast.html>).

The above discussion is intentionally heuristic and somewhat vague because many of the issues involved are technical and not particularly illuminating. My main point is an appreciation for the detailed and precise physics which goes into computing microwave background

fluctuations. However, all of this formalism should not obscure several basic physical processes which determine the ultimate form of the fluctuations. A widespread understanding of most of the physical processes detailed below followed from a seminal paper by Hu and Sugiyama (1994), a classic of the microwave background literature.

### 3.3. Tight coupling

Two basic time scales enter into the evolution of the microwave background. The first is the photon scattering time scale  $t_s$ , the mean time between Thomson scatterings. The other is the expansion time scale of the universe,  $H^{-1}$ , where  $H = \dot{a}/a$  is the Hubble parameter. At temperatures significantly greater than 0.5 eV, hydrogen and helium are completely ionized and  $t_s \ll H^{-1}$ . The Thomson scatterings which couple the electrons and photons occur much more rapidly than the expansion of the universe; as a result, the baryons and photons behave as a single “tightly coupled” fluid. During this period, the fluctuations in the photons mirror the fluctuations in the baryons. (Note that recombination occurs at around 0.5 eV rather than 13.6 eV because of the huge photon-baryon ratio; the universe contains somewhere around  $10^9$  photons for each baryon, as we know from primordial nucleosynthesis. It is a useful exercise to work out the approximate recombination temperature.)

The photon distribution function for scalar perturbations can be written as  $\Theta(\mathbf{k}, \mu, t)$  where  $\mu = \hat{\mathbf{k}} \cdot \hat{\mathbf{n}}$  and the scalar character of the fluctuations guarantees the distribution cannot have any azimuthal directional dependence. (The azimuthal dependence for vector and tensor perturbations can also be included in a similar decomposition). The moments of the distribution are defined as

$$\Theta(\mathbf{k}, \mu, t) = \sum_{l=0}^{\infty} (-i)^l \Theta_l(\mathbf{k}, t) P_l(\mu); \quad (1)$$

sometimes other normalizations are used. Tight coupling implies that  $\Theta_l = 0$  for  $l > 1$ . Physically, the  $l = 0$  moment corresponds to the photon energy density perturbation, while  $l = 1$  corresponds to the bulk velocity. During tight coupling, these two moments must match the baryon density and velocity perturbations. Any higher moments rapidly decay due to the isotropizing effect of Thomson scattering; this follows immediately from the photon Boltzmann equation.

### 3.4. Free streaming

In the other regime, for temperatures significantly lower than 0.5 eV,  $t_s \gg H^{-1}$  and photons on average never scatter again until the present time. This is known as the “free streaming” epoch. Since the radiation is no longer tightly coupled to the electrons, all higher moments in the radiation field develop as the photons propagate. In a flat background spacetime, the exact solution is simple to derive. After scattering ceases, the photons evolve according to the Liouville equation

$$\Theta' + ik\mu\Theta = 0 \tag{2}$$

with the trivial solution

$$\Theta(\mathbf{k}, \mu, \eta) = e^{-ik\mu(\eta-\eta_*)}\Theta(\mathbf{k}, \mu, \eta_*), \tag{3}$$

where we have converted to conformal time defined by  $d\eta = dt/a(t)$  and  $\eta_*$  corresponds to the time at which free streaming begins. Taking moments of both sides results in

$$\Theta_l(\mathbf{k}, \eta) = (2l + 1) [\Theta_0(\mathbf{k}, \eta_*)j_l(k\eta - k\eta_*) + \Theta_1(\mathbf{k}, \eta_*)j'_l(k\eta - k\eta_*)] \tag{4}$$

with  $j_l$  a spherical Bessel function. The process of free streaming essentially maps spatial variations in the photon distribution at the last scattering surface (wavenumber  $k$ ) into angular variations on the sky today (moment  $l$ ).

### 3.5. Diffusion damping

In the intermediate regime during recombination,  $t_s \simeq H^{-1}$ . Photons propagate a characteristic distance  $L_D$  during this time. Since some scattering is still occurring, baryons experience a drag from the photons as long as the ionization fraction is appreciable. A second-order perturbation analysis shows that the result is damping of baryon fluctuations on scales below  $L_D$ , known as Silk damping or diffusion damping. This effect can be modelled by the replacement

$$\Theta_0(\mathbf{k}, \eta_*) \rightarrow \Theta_0(\mathbf{k}, \eta_*)e^{-(kL_D)^2} \tag{5}$$

although detailed calculations are needed to define  $L_D$  precisely. As a result of this damping, microwave background fluctuations are exponentially suppressed on angular scales significantly smaller than a degree.

### 3.6. The resulting power spectrum

The fluctuations in the universe are assumed to arise from some random statistical process. We are not interested in the exact pattern of fluctuations we see from our vantage point, since this is only a single realization of the process. Rather, a theory of cosmology predicts an underlying distribution, of which our visible sky is a single statistical realization. The most basic statistic describing fluctuations is their power spectrum. A temperature map on the sky  $T(\hat{\mathbf{n}})$  is conventionally expanded in spherical harmonics,

$$\frac{T(\hat{\mathbf{n}})}{T_0} = 1 + \sum_{l=1}^{\infty} \sum_{m=-l}^l a_{(lm)}^{\text{T}} Y_{(lm)}(\hat{\mathbf{n}}) \quad (6)$$

where

$$a_{(lm)}^{\text{T}} = \frac{1}{T_0} \int d\hat{\mathbf{n}} T(\hat{\mathbf{n}}) Y_{(lm)}^*(\hat{\mathbf{n}}) \quad (7)$$

are the temperature multipole coefficients and  $T_0$  is the mean CMB temperature. The  $l = 1$  term in Eq. (6) is indistinguishable from the kinematic dipole and is normally ignored. The temperature angular power spectrum  $C_l$  is then given by

$$\langle a_{(lm)}^{\text{T}*} a_{(l'm')}^{\text{T}} \rangle = C_l^{\text{T}} \delta_{ll'} \delta_{mm'}, \quad (8)$$

where the angled brackets represent an average over statistical realizations of the underlying distribution. Since we have only a single sky to observe, an unbiased estimator of  $C_l$  is constructed as

$$\hat{C}_l^{\text{T}} = \frac{1}{2l+1} \sum_{m=-l}^l a_{lm}^{\text{T}*} a_{lm}^{\text{T}}. \quad (9)$$

The statistical uncertainty in estimating  $C_l^{\text{T}}$  by a sum of  $2l+1$  terms is known as “cosmic variance”. The constraints  $l = l'$  and  $m = m'$  follow from the assumption of statistical isotropy:  $C_l^{\text{T}}$  must be independent of the orientation of the coordinate system used for the harmonic expansion. These conditions can be verified via an explicit rotation of the coordinate system.

A given cosmological theory will predict  $C_l^{\text{T}}$  as a function of  $l$ , which can be obtained from evolving the temperature distribution function as described above. This prediction can then be compared with data from measured temperature differences on the sky. Figure 1 shows a typical temperature power spectrum from the inflationary class of models, described in more detail below. The distinctive sequence of peaks arise from coherent acoustic oscillations in the fluid during the tight coupling epoch and are of great importance in precision tests of cosmological models; these peaks will be discussed in Sec. 5. The effect of diffusion damping is clearly visible in the decreasing power above  $l = 1000$ . When viewing angular power

spectrum plots in multipole space, keep in mind that  $l = 200$  corresponds approximately to fluctuations on angular scales of a degree, and the angular scale is inversely proportional to  $l$ . The vertical axis is conventionally plotted as  $l(l+1)C_l^T$  because the Sachs-Wolfe temperature fluctuations from a scale-invariant spectrum of density perturbations appears as a horizontal line on such a plot.

## 4. Physics of Polarization Fluctuations

In addition to temperature fluctuations, the simple physics of decoupling inevitably leads to non-zero polarization of the microwave background radiation as well, although quite generically the polarization fluctuations are expected to be significantly smaller than the temperature fluctuations. This section reviews the physics of polarization generation and its description. For a more detailed pedagogical discussion of microwave background polarization, see Kosowsky (1999), from which this section is excerpted.

### 4.1. Stokes parameters

Polarized light is conventionally described in terms of the Stokes parameters, which are presented in any optics text. If a monochromatic electromagnetic wave propagating in the  $z$ -direction has an electric field vector at a given point in space given by

$$E_x = a_x(t) \cos[\omega_0 t - \theta_x(t)], \quad E_y = a_y(t) \cos[\omega_0 t - \theta_y(t)], \quad (10)$$

then the Stokes parameters are defined as the following time averages:

$$I \equiv \langle a_x^2 \rangle + \langle a_y^2 \rangle; \quad (11)$$

$$Q \equiv \langle a_x^2 \rangle - \langle a_y^2 \rangle; \quad (12)$$

$$U \equiv \langle 2a_x a_y \cos(\theta_x - \theta_y) \rangle; \quad (13)$$

$$V \equiv \langle 2a_x a_y \sin(\theta_x - \theta_y) \rangle. \quad (14)$$

The averages are over times long compared to the inverse frequency of the wave. The parameter  $I$  gives the intensity of the radiation which is always positive and is equivalent to the temperature for blackbody radiation. The other three parameters define the polarization state of the wave and can have either sign. Unpolarized radiation, or “natural light,” is described by  $Q = U = V = 0$ .

The parameters  $I$  and  $V$  are physical observables independent of the coordinate system, but  $Q$  and  $U$  depend on the orientation of the  $x$  and  $y$  axes. If a given wave is described

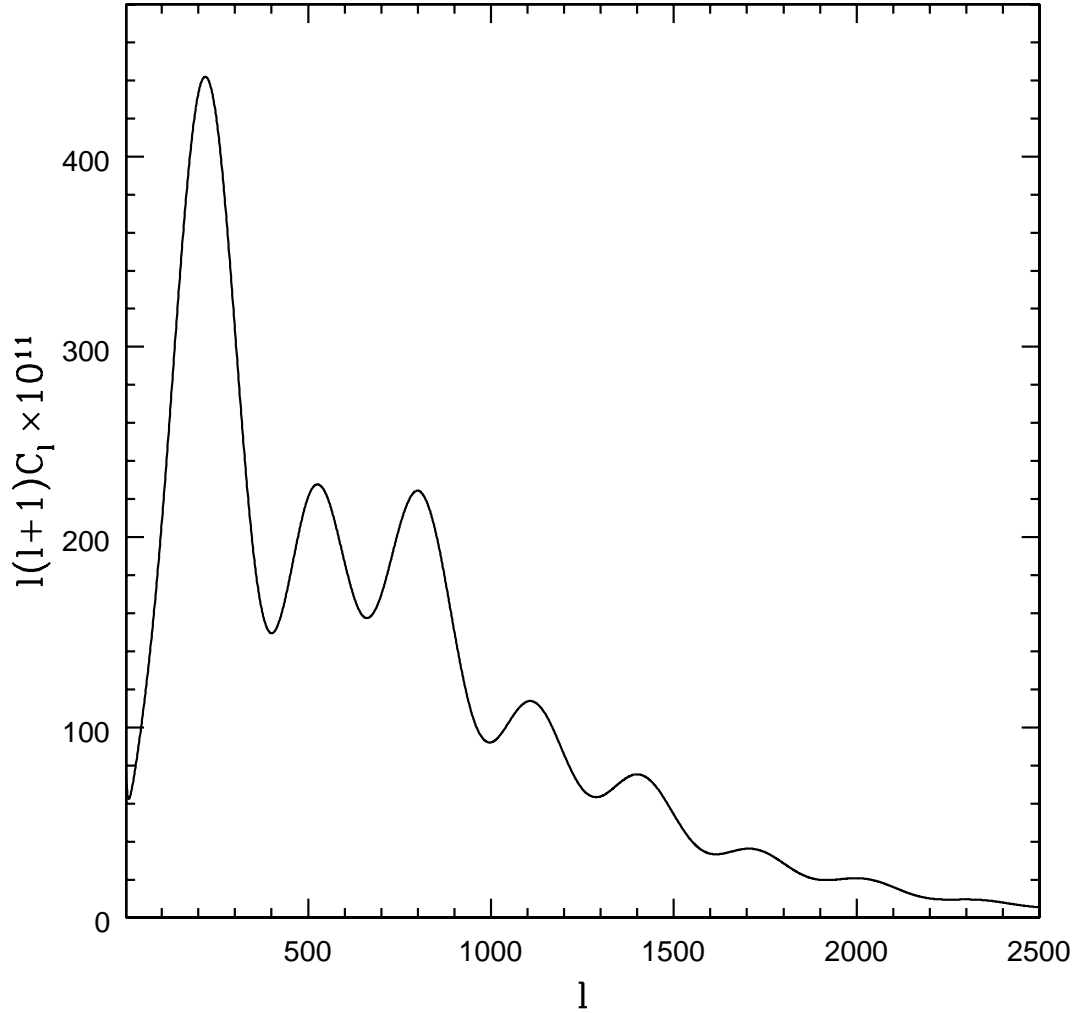


Fig. 1.— The temperature angular power spectrum for a cosmological model with mass density  $\Omega_0 = 0.3$ , vacuum energy density  $\Omega_\Lambda = 0.7$ , Hubble parameter  $h = 0.7$ , and a scale-invariant spectrum of primordial adiabatic perturbations.

by the parameters  $Q$  and  $U$  for a certain orientation of the coordinate system, then after a rotation of the  $x - y$  plane through an angle  $\phi$ , it is straightforward to verify that the same wave is now described by the parameters

$$\begin{aligned} Q' &= Q \cos(2\phi) + U \sin(2\phi), \\ U' &= -Q \sin(2\phi) + U \cos(2\phi). \end{aligned} \tag{15}$$

From this transformation it is easy to see that the quantity  $P^2 \equiv Q^2 + U^2$  is invariant under rotation of the axes, and the angle

$$\alpha \equiv \frac{1}{2} \tan^{-1} \frac{U}{Q} \tag{16}$$

defines a constant orientation parallel to the electric field of the wave. The Stokes parameters are a useful description of polarization because they are *additive* for incoherent superposition of radiation; note this is not true for the magnitude or orientation of polarization. Note that the transformation law in Eq. (15) is characteristic not of a vector but of the second-rank *tensor*

$$\rho = \frac{1}{2} \begin{pmatrix} I + Q & U - iV \\ U + iV & I - Q \end{pmatrix}, \tag{17}$$

which also corresponds to the quantum mechanical density matrix for an ensemble of photons (Kosowsky 1996). In kinetic theory, the photon distribution function  $f(\mathbf{x}, \mathbf{p}, t)$  discussed in Sec. 3.2 must be generalized to  $\rho_{ij}(\mathbf{x}, \mathbf{p}, t)$ , corresponding to this density matrix.

## 4.2. Thomson scattering and the quadrupolar source

Non-zero linear polarization in the microwave background is generated around decoupling because the Thomson scattering which couples the radiation and the electrons is not isotropic but varies with the scattering angle. The total scattering cross-section, defined as the radiated intensity per unit solid angle divided by the incoming intensity per unit area, is given by

$$\frac{d\sigma}{d\Omega} = \frac{3\sigma_T}{8\pi} |\hat{\varepsilon}' \cdot \hat{\varepsilon}|^2 \tag{18}$$

where  $\sigma_T$  is the total Thomson cross section and the vectors  $\hat{\varepsilon}$  and  $\hat{\varepsilon}'$  are unit vectors in the planes perpendicular to the propagation directions which are aligned with the outgoing and incoming polarization, respectively. This scattering cross-section can give no net circular polarization, so  $V = 0$  for cosmological perturbations and will not be discussed further. Measurements of  $V$  polarization can be used as a diagnostic of systematic errors or microwave foreground emission.

It is a straightforward but slightly involved exercise to show that the above relations imply that an incoming unpolarized radiation field with the multipole expansion Eq. (6) incident upon an electron in a sample volume with cross-section  $\sigma_B$  will be Thomson scattered into an outgoing radiation field from the sample volume with Stokes parameters

$$Q(\hat{\mathbf{n}}) - iU(\hat{\mathbf{n}}) = \frac{3\sigma_T}{8\pi\sigma_B} \sqrt{\frac{\pi}{5}} a_{20} \sin^2 \beta \quad (19)$$

if the incoming radiation propagating in a given direction has rotational symmetry around its direction of propagation, as will hold for individual Fourier modes of scalar perturbations. Explicit expressions for the general case of no symmetry can be derived in terms of Wigner D-symbols (Kosowsky 1999).

In simple and general terms, unpolarized incoming radiation will be Thomson scattered into linearly polarized radiation if and only if the incoming radiation has a non-zero quadrupolar directional dependence. This single fact is sufficient to understand the fundamental physics behind polarization of the microwave background. During the tight-coupling epoch, the radiation field has only monopole and dipole directional dependences as explained above; therefore, scattering can produce no net polarization and the radiation remains unpolarized. As tight coupling begins to break down as recombination begins, a quadrupole moment of the radiation field will begin to grow due to free streaming of the photons. Polarization is generated during the brief interval when a significant quadrupole moment of the radiation has built up, but the scattering electrons have not yet all recombined. Note that if the universe recombined instantaneously, the net polarization of the microwave background would be zero. Due to this competition between the quadrupole source building up and the density of scatterers declining, the amplitude of polarization in the microwave background is generically suppressed by an order of magnitude compared to the temperature fluctuations.

Before polarization generation commences, the temperature fluctuations have either a monopole dependence, corresponding to density perturbations, or a dipole dependence, corresponding to velocity perturbations. A straightforward solution to the photon free-streaming equation (in terms of spherical Bessel functions) shows that for Fourier modes with wavelengths large compared to a characteristic thickness of the surface of last scattering, the quadrupole contribution through the last scattering surface is dominated by the velocity fluctuations in the temperature, not the density fluctuations. This makes intuitive sense: the dipole fluctuations can free stream directly into the quadrupole, but the monopole fluctuations must stream through the dipole first. This conclusion breaks down on small scales where either monopole or dipole can be the dominant quadrupole source, but numerical computations show that on scales of interest for microwave background fluctuations, the dipole temperature fluctuations are always the dominant source of quadrupole fluctuations at the

surface of last scattering. Therefore, polarization fluctuations reflect mainly velocity perturbations at last scattering, in contrast to temperature fluctuations which predominantly reflect density perturbations.

### 4.3. Harmonic expansions and power spectra

Just as the temperature on the sky can be expanded into spherical harmonics, facilitating the computation of the angular power spectrum, so can the polarization. The situation is formally parallel, although in practice it is more complicated: while the temperature is a scalar quantity, the polarization is a second-rank tensor. We can define a polarization tensor with the correct transformation properties, Eq. (15), as

$$P_{ab}(\hat{\mathbf{n}}) = \frac{1}{2} \begin{pmatrix} Q(\hat{\mathbf{n}}) & -U(\hat{\mathbf{n}}) \sin \theta \\ -U(\hat{\mathbf{n}}) \sin \theta & -Q(\hat{\mathbf{n}}) \sin^2 \theta \end{pmatrix}. \quad (20)$$

The dependence on the Stokes parameters is the same as for the density matrix, Eq. 17; the extra factors are convenient because the usual spherical coordinate basis is orthogonal but not orthonormal. This tensor quantity must be expanded in terms of tensor spherical harmonics which preserve the correct transformation properties. We assume a complete set of orthonormal basis functions for symmetric trace-free  $2 \times 2$  tensors on the sky,

$$\frac{P_{ab}(\hat{\mathbf{n}})}{T_0} = \sum_{l=2}^{\infty} \sum_{m=-l}^l [a_{(lm)}^G Y_{(lm)ab}^G(\hat{\mathbf{n}}) + a_{(lm)}^C Y_{(lm)ab}^C(\hat{\mathbf{n}})], \quad (21)$$

where the expansion coefficients are given by

$$a_{(lm)}^G = \frac{1}{T_0} \int d\hat{\mathbf{n}} P_{ab}(\hat{\mathbf{n}}) Y_{(lm)}^{G*ab*}(\hat{\mathbf{n}}), \quad (22)$$

$$a_{(lm)}^C = \frac{1}{T_0} \int d\hat{\mathbf{n}} P_{ab}(\hat{\mathbf{n}}) Y_{(lm)}^{C*ab*}(\hat{\mathbf{n}}), \quad (23)$$

which follow from the orthonormality properties

$$\int d\hat{\mathbf{n}} Y_{(lm)ab}^{G*}(\hat{\mathbf{n}}) Y_{(l'm')ab}^G(\hat{\mathbf{n}}) = \int d\hat{\mathbf{n}} Y_{(lm)ab}^{C*}(\hat{\mathbf{n}}) Y_{(l'm')ab}^C(\hat{\mathbf{n}}) = \delta_{ll'} \delta_{mm'}, \quad (24)$$

$$\int d\hat{\mathbf{n}} Y_{(lm)ab}^{G*}(\hat{\mathbf{n}}) Y_{(l'm')ab}^C(\hat{\mathbf{n}}) = 0. \quad (25)$$

These tensor spherical harmonics are not as exotic as they might sound; they are used extensively in the theory of gravitational radiation, where they naturally describe the radiation multipole expansion. Tensor spherical harmonics are similar to vector spherical

harmonics used to represent electromagnetic radiation fields, familiar from Chapter 16 of Jackson (1975). Explicit formulas for tensor spherical harmonics can be derived via various algebraic and group theoretic methods; see Thorne (1980) for a complete discussion. A particularly elegant and useful derivation of the tensor spherical harmonics (along with the vector spherical harmonics as well) is provided by differential geometry: the harmonics can be expressed as covariant derivatives of the usual spherical harmonics with respect to an underlying manifold of a two-sphere (i.e., the sky). This construction has been carried out explicitly and applied to the microwave background polarization (Kamionkowski, Kosowsky, and Stebbins 1996).

The existence of two sets of basis functions, labeled here by “G” and “C”, is due to the fact that the symmetric traceless  $2 \times 2$  tensor describing linear polarization is specified by two independent parameters. In two dimensions, any symmetric traceless tensor can be uniquely decomposed into a part of the form  $A_{;ab} - (1/2)g_{ab}A_{;c}{}^c$  and another part of the form  $B_{;ac}\epsilon^c{}_b + B_{;bc}\epsilon^c{}_a$  where  $A$  and  $B$  are two scalar functions and semicolons indicate covariant derivatives. This decomposition is quite similar to the decomposition of a vector field into a part which is the gradient of a scalar field and a part which is the curl of a vector field; hence we use the notation G for “gradient” and C for “curl”. In fact, this correspondence is more than just cosmetic: if a linear polarization field is visualized in the usual way with headless “vectors” representing the amplitude and orientation of the polarization, then the G harmonics describe the portion of the polarization field which has no handedness associated with it, while the C harmonics describe the other portion of the field which does have a handedness (just as with the gradient and curl of a vector field). Note that Zaldarriaga and Seljak (1997) label these harmonics E and B, with a slightly different normalization than defined here (see Kamionkowski *et al.* 1996).

We now have three sets of multipole moments,  $a_{(lm)}^T$ ,  $a_{(lm)}^G$ , and  $a_{(lm)}^C$ , which fully describe the temperature/polarization map of the sky. These moments can be combined quadratically into various power spectra analogous to the temperature  $C_l^T$ . Statistical isotropy implies that

$$\begin{aligned}
 \langle a_{(lm)}^{T*} a_{(l'm')}^T \rangle &= C_l^T \delta_{ll'} \delta_{mm'}, & \langle a_{(lm)}^{G*} a_{(l'm')}^G \rangle &= C_l^G \delta_{ll'} \delta_{mm'}, \\
 \langle a_{(lm)}^{C*} a_{(l'm')}^C \rangle &= C_l^C \delta_{ll'} \delta_{mm'}, & \langle a_{(lm)}^{T*} a_{(l'm')}^G \rangle &= C_l^{TG} \delta_{ll'} \delta_{mm'}, \\
 \langle a_{(lm)}^{T*} a_{(l'm')}^C \rangle &= C_l^{TC} \delta_{ll'} \delta_{mm'}, & \langle a_{(lm)}^{G*} a_{(l'm')}^C \rangle &= C_l^{GC} \delta_{ll'} \delta_{mm'},
 \end{aligned} \tag{26}$$

where the angle brackets are an average over all realizations of the probability distribution for the cosmological initial conditions. Simple statistical estimators of the various  $C_l$ 's can be constructed from maps of the microwave background temperature and polarization.

For fluctuations with gaussian random distributions (as predicted by the simplest inflation models), the statistical properties of a temperature/polarization map are specified fully by these six sets of multipole moments. In addition, the scalar spherical harmonics

$Y_{(lm)}$  and the G tensor harmonics  $Y_{(lm)ab}^G$  have parity  $(-1)^l$ , but the C harmonics  $Y_{(lm)ab}^C$  have parity  $(-1)^{l+1}$ . If the large-scale perturbations in the early universe were invariant under parity inversion, then  $C_l^{\text{TC}} = C_l^{\text{GC}} = 0$ . So generally, microwave background fluctuations are characterized by the four power spectra  $C_l^{\text{T}}$ ,  $C_l^{\text{G}}$ ,  $C_l^{\text{C}}$ , and  $C_l^{\text{TG}}$ . These The end result of the numerical computations described in Sec. 3.2 above are these power spectra. Polarization power spectra  $C_l^{\text{G}}$  and  $C_l^{\text{TG}}$  for scalar perturbations in a typical inflation-like cosmological model, generated with the CMBFAST code (Seljak and Zaldarriaga 1996), are displayed in Fig. 2. The temperature power spectrum in Fig. 1 and the polarization power spectra in Fig. 2 come from the same cosmological model. The physical source of the features in the power spectra is discussed in the next section, followed by a discussion of how cosmological parameters can be determined to high precision via detailed measurements of the microwave background power spectra.

## 5. Acoustic Oscillations

Before decoupling, the matter in the universe has significant pressure because it is tightly coupled to radiation. This pressure counteracts any tendency for matter to collapse gravitationally. Formally, the Jeans mass is greater than the mass within a horizon volume for times earlier than decoupling. During this epoch, density perturbations will set up standing acoustic waves in the plasma. Under certain conditions, these waves leave a distinctive imprint on the power spectrum of the microwave background, which in turn provides the basis for precision constraints on cosmological parameters. This section reviews the basics of the acoustic oscillations.

### 5.1. An oscillator equation

In their classic 1996 paper, Hu and Sugiyama transformed the basic equations describing the evolution of perturbations into an oscillator equation. Combining the zeroth moment of the photon Boltzmann equation with the baryon Euler equation for a given  $k$ -mode in the tight-coupling approximation (mean baryon velocity equals mean radiation velocity) gives

$$\ddot{\Theta}_0 + H \frac{R}{1+R} \dot{\Theta}_0 + k^2 c_s^2 \Theta_0 = -\ddot{\Phi} - H \frac{R}{1+R} \dot{\Phi} - \frac{1}{3} k^2 \Psi, \quad (27)$$

where  $\Theta_0$  is the zeroth moment of the temperature distribution function (proportional to the photon density perturbation),  $R = 3\rho_b/4\rho_\gamma$  is proportional to the scale factor  $a$ ,  $H = \dot{a}/a$  is the conformal Hubble parameter, and the sound speed is given by  $c_s^2 = 1/(3 + 3R)$ . (All overdots are derivatives with respect to conformal time.)  $\Phi$  and  $\Psi$  are the scalar metric

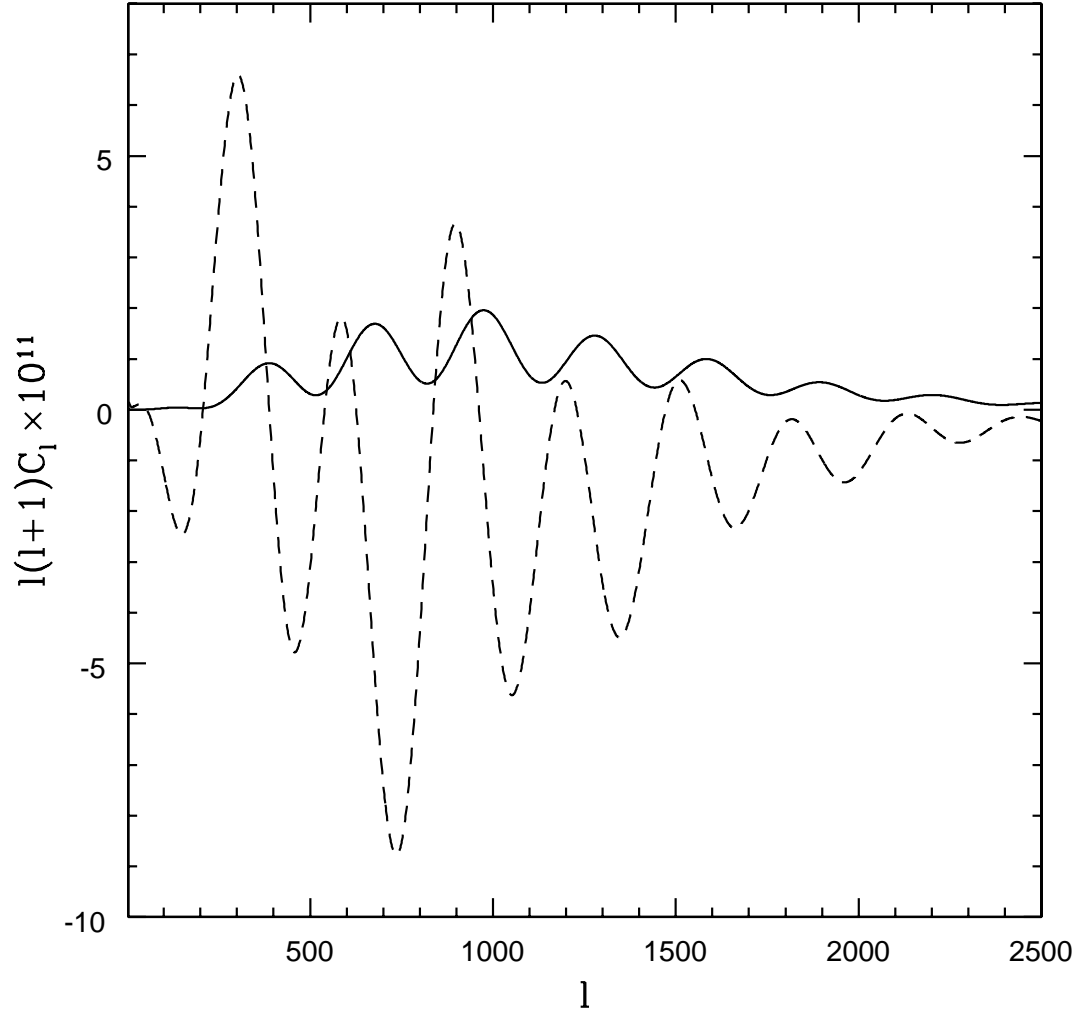


Fig. 2.— The G polarization power spectrum (solid line) and the cross-power TG between temperature and polarization (dashed line), for the same model as in Fig. 1.

perturbations in the Newtonian gauge; if we neglect the anisotropic stress, which is generally small in conventional cosmological scenarios, then  $\Psi = -\Phi$ . But the details are not very important. The equation represents damped, driven oscillations of the radiation density, and the various physical effects are easily identified. The second term on the left side is the damping of oscillations due to the expansion of the universe. The third term on the left side is the restoring force due to the pressure, since  $c_s^2 = dP/d\rho$ . On the right side, the first two terms depend on the time variation of the gravitational potentials, so these two are the source of the Integrated Sachs-Wolfe effect. The final term on the right side is the driving term due to the gravitational potential perturbations. As Hu and Sugiyama emphasized, these damped, driven acoustic oscillations account for all of the structure in the microwave background power spectrum.

A WKB approximation to the homogeneous equation with no driving source terms gives the two oscillation modes (Hu and Sugiyama 1996)

$$\Theta_0(k, \eta) \propto \begin{cases} (1 + R)^{-1/4} \cos kr_s(\eta) \\ (1 + R)^{-1/4} \sin kr_s(\eta) \end{cases} \quad (28)$$

where the sound horizon  $r_s$  is given by

$$r_s(\eta) \equiv \int_0^\eta c_s(\eta') d\eta'. \quad (29)$$

Note that at times well before matter-radiation equality, the sound speed is essentially constant,  $c_s = 1/\sqrt{3}$ , and the sound horizon is simply proportional to the causal horizon. In general, any perturbation with wavenumber  $k$  will set up an oscillatory behavior in the primordial plasma described by a linear combination of the two modes in Eq. (28). The relative contribution of the modes will be determined by the initial conditions describing the perturbation.

Equation (27) appears to be simpler than it actually is, because  $\Phi$  and  $\Psi$  are the total gravitational potentials due to all matter and radiation, including the photons which the left side is describing. In other words, the right side of the equation contains an implicit dependence on  $\Theta_0$ . At the expense of pedagogical transparency, this situation can be remedied by considering separately the potential from the photon-baryon fluid and the potential from the truly external sources, the dark matter and neutrinos. This split has been performed by Hu and White (1996). The resulting equation, while still an oscillator equation, is much more complicated, but must be used for a careful physical analysis of acoustic oscillations.

## 5.2. Initial conditions

The initial conditions for radiation perturbations for a given wavenumber  $k$  can be broken into two categories, according to whether the gravitational potential perturbation from the baryon-photon fluid,  $\Phi_{b\gamma}$ , is nonzero or zero as  $\eta \rightarrow 0$ . The former case is known as “adiabatic” (which is somewhat of a misnomer since adiabatic technically refers to a property of a time-dependent process) and implies that  $n_b/n_\gamma$ , the ratio of baryon to photon number densities, is a constant in space. This case must couple to the cosine oscillation mode since it requires  $\Theta_0 \neq 0$  as  $\eta \rightarrow 0$ . The simplest (i.e. single-field) models of inflation produce perturbations with adiabatic initial conditions.

The other case is termed “isocurvature” since the fluid gravitational potential perturbation  $\Phi_{b\gamma}$ , and hence the perturbations to the spatial curvature, are zero. In order to arrange such a perturbation, the baryon and photon densities must vary in such a way that they compensate each other:  $n_b/n_\gamma$  varies, and thus these perturbations are in entropy, not curvature. At an early enough time, the temperature perturbation in a given  $k$  mode must arise entirely from the Sachs-Wolfe effect, and thus isocurvature perturbations couple to the sine oscillation mode. These perturbations arise from causal processes like phase transitions: a phase transition cannot change the energy density of the universe from point to point, but it can alter the relative entropy between various types of matter depending on the values of the fields involved. The potentially most interesting cause of isocurvature perturbations is multiple dynamical fields in inflation. The fields will exchange energy during inflation, and the field values will vary stochastically between different points in space at the end of the phase transition, generically giving isocurvature along with adiabatic perturbations (Polarski and Starobinsky 1994).

The numerical problem of setting initial conditions is somewhat tricky. The general problem of evolving perturbations involves linear evolution equations for around a dozen variables, outlined in Sec. 3.2. Setting the correct initial conditions involves specifying the value of each variable in the limit as  $\eta \rightarrow 0$ . This is difficult for two reasons: the equations are singular in this limit, and the equations become increasingly numerically stiff in this limit. Simply using the leading-order asymptotic behavior for all of the variables is only valid in the high-temperature limit. Since the equations are stiff, small departures from this limiting behavior in any of the variables can lead to numerical instability until the equations evolve to a stiff solution, and this numerical solution does not necessarily correspond to the desired initial conditions. Numerical techniques for setting the initial conditions to high accuracy at temperatures are currently being developed.

### 5.3. Coherent oscillations

The characteristic “acoustic peaks” which appear in Figure 1 arise from acoustic oscillations which are phase coherent: at some point in time, the phases of all of the acoustic oscillations were the same. This requires the same initial condition for *all*  $k$ -modes, including those with wavelengths longer than the horizon. Such a condition arises naturally for inflationary models, but is very hard to reproduce in models producing perturbations causally on scales smaller than the horizon. Defect models, for example, produce acoustic oscillations, but the oscillations generically have incoherent phases and thus display no peak structure in their power spectrum (Seljak *et al.* 1997). Simple models of inflation which produce only adiabatic perturbations insure that all perturbations have the same phase at  $\eta = 0$  because all of the perturbations are in the cosine mode of Eq. (28).

A glance at the  $k$  dependence of the adiabatic perturbation mode reveals how the coherent peaks are produced. The microwave background images the radiation density at a fixed time; as a function of  $k$ , the density varies like  $\cos(kr_s)$ , where  $r_s$  is fixed. Physically, on scales much larger than the horizon at decoupling, a perturbation mode has not had enough time to evolve. At a particular smaller scale, the perturbation mode evolves to its maximum density in potential wells, at which point decoupling occurs. This is the scale reflected in the first acoustic peak in the power spectrum. Likewise, at a particular still smaller scale, the perturbation mode evolves to its maximum density in potential wells and then turns around, evolving to its minimum density in potential wells; at that point, decoupling occurs. This scale corresponds to that of the second acoustic peak. (Since the power spectrum is the square of the temperature fluctuation, both compressions and rarefactions in potential wells correspond to peaks in the power spectrum.) Each successive peak represents successive oscillations, with the scales of odd-numbered peaks corresponding to those perturbation scales which have ended up compressed in potential wells at the time of decoupling, while the even-numbered peaks correspond to the perturbation scales which are rarefied in potential wells at decoupling. If the perturbations are not phase coherent, then the phase of a given  $k$ -mode at decoupling is not well defined, and the power spectrum just reflects some mean fluctuation power at that scale.

In practice, two additional effects must be considered: a given scale in  $k$ -space is mapped to a range of  $l$ -values; and radiation velocities as well as densities contribute to the power spectrum. The first effect broadens out the peaks, while the second fills in the valleys between the peaks since the velocity extrema will be exactly out of phase with the density extrema. The amplitudes of the peaks in the power spectrum are also suppressed by Silk damping, as mentioned in Sec. 3.5.

#### 5.4. The effect of baryons

The mass of the baryons creates a distinctive signature in the acoustic oscillations (Hu and Sugiyama 1996). The zero-point of the oscillations is obtained by setting  $\Theta_0$  constant in Eq. (27): the result is

$$\Theta_0 \simeq \frac{1}{3c_s^2}\Phi = (1 + a)\Phi. \quad (30)$$

The photon temperature  $\Theta_0$  is not itself observable, but must be combined with the gravitational redshift to form the “apparent temperature”  $\Theta_0 - \Phi$ , which oscillates around  $a\Phi$ . If the oscillation amplitude is much larger than  $a\Phi = 3\rho_b\Phi/4\rho_\gamma$ , then the oscillations are effectively about the mean temperature. The positive and negative oscillations are of the same amplitude, so when the apparent temperature is squared to form the power spectrum, all of the peaks have the same height. On the other hand, if the baryons contribute a significant mass so that  $a\Phi$  is a significant fraction of the oscillation amplitude, then the zero point of the oscillations are displaced, and when the apparent temperature is squared to form the power spectrum, the peaks arising from the positive oscillations are higher than the peaks from the negative oscillations. If  $a\Phi$  is larger than the amplitude of the oscillations, then the power spectrum peaks corresponding to the negative oscillations disappear entirely. The physical interpretation of this effect is that the baryon mass deepens the potential well in which the baryons are oscillating, increasing the compression of the plasma compared to the case with less baryon mass. In short, as the baryon density increases, the power spectrum peaks corresponding to compressions in potential wells get higher, while the alternating peaks corresponding to rarefactions get lower. This alternating peak height signature is a distinctive signature of baryon mass, and allows the precise determination of the cosmological baryon density with the measurement of the first several acoustic peak heights.

### 6. Cosmological Models and Constraints

The cosmological interpretation of a measured microwave background power spectrum requires, to some extent, the introduction of a particular space of models. A very simple, broad, and well-motivated set of models are motivated by inflation: a universe described by a homogeneous and isotropic background with phase-coherent, power-law initial perturbations which evolve freely. This model space excludes, for example, perturbations caused by topological defects or other “stiff” sources, arbitrary initial power spectra, or any departures from the standard background cosmology. This set of models has the twin virtues of being relatively simple to calculate and best conforming to current power spectrum measurements. (In fact, most competing cosmological models, like those employing cosmic defects to make

structure, are essentially ruled out by current microwave background and large-scale structure measurements.) This section will describe the parameters defining the model space and discuss the extent to which the parameters can be constrained through the microwave background.

### 6.1. A space of models

The parameters defining the model space can be broken into three types: cosmological parameters describing the background space-time; parameters describing the initial conditions; and other parameters describing miscellaneous additional physical effects. Background cosmological parameters are:

- $\Omega$ , the ratio of the total energy density to the critical density  $\rho_c = 8\pi/3H^2$ . This parameter determines the spatial curvature of the universe:  $\Omega = 1$  is a flat universe with critical density. Smaller values of  $\Omega$  correspond to a negative spatial curvature, while larger values correspond to positive curvature. Current microwave background measurements constrain  $\Omega$  to be roughly within the range 0.8 to 1.2, consistent with a critical-density universe.
- $\Omega_b$ , the ratio of the baryon density to the critical density. Observations of the abundance of deuterium in high redshift gas clouds and comparison with predictions from primordial nucleosynthesis place strong constraints on this parameter (Tytler *et al.* 2000).
- $\Omega_m$ , the ratio of the dark matter density to the critical density. Dynamical constraints, gravitational lensing, cluster abundances, and numerous other lines of evidence all point to a total matter density in the neighborhood of  $\Omega_0 = \Omega_m + \Omega_b = 0.3$ .
- $\Omega_\Lambda$ , the ratio of vacuum energy density  $\Lambda$  to the critical density. This is the notorious cosmological constant. Several years ago, almost no cosmologist advocated a cosmological constant; now almost every cosmologist accepts its existence. The shift was precipitated by the Type Ia supernova Hubble diagram (Perlmutter *et al.* 1999, Riess *et al.* 1998) which shows an apparent acceleration in the expansion of the universe. Combined with strong constraints on  $\Omega$ , a cosmological constant now seems unavoidable, although high-energy theorists have a difficult time accepting it. Strong gravitational lensing of quasars places upper limits on  $\Omega_\Lambda$  (Falco *et al.* 1998).
- The present Hubble parameter  $h$ , in units of 100 km/s/Mpc. Distance ladder measurements (Mould *et al.* 2000) and supernova Ia measurements (Riess *et al.* 1998) give

consistent estimates for  $h$  of around 0.70, with systematic errors on the order of 10%.

- Optionally, further parameters describing additional contributions to the energy density of the universe. An example is “quintessence” models (Caldwell *et al.* 1998) which add one or more scalar fields to the universe.

Parameters describing the initial conditions are:

- The amplitude of fluctuations  $Q$ , often defined at the quadrupole scale. COBE fixed this amplitude to high accuracy (Bennett *et al.* 1996).
- The power law index  $n$  of initial adiabatic density fluctuations. The scale-invariant Harrison-Zeldovich spectrum is  $n = 1$ . Comparison of microwave background and large-scale structure measurements shows that  $n$  is close to unity.
- The relative contribution of tensor and scalar perturbations  $r$ , usually defined as the ratio of the power at  $l = 2$  from each type of perturbation. The fact that prominent features are seen in the power spectrum (presumably arising from scalar density perturbations) limits the power spectrum contribution of tensor perturbations to roughly 20% of the scalar amplitude.
- The power law index  $n_T$  of tensor perturbations. Unfortunately, tensor power spectra are generally defined so that  $n_T = 0$  corresponds to scale invariant, in contrast to the scalar case.
- Optionally, more parameters describing either departures of the scalar perturbations from a power law (e.g. Kosowsky and Turner 1995) or a small admixture of isocurvature perturbations.

Other miscellaneous parameters include:

- A significant neutrino mass  $m_\nu$ . None of the current neutrino oscillation results favor a cosmologically interesting neutrino mass.
- The effective number of neutrino species  $N_\nu$ . This quantity includes any particle species which is relativistic when it decouples or can model entropy production prior to last scattering.
- The redshift of reionization,  $z_r$ . Spectra of quasars at redshift  $z = 5$  show that the universe has been reionized at least since then.

A realistic parameter analysis might include at least 8 free parameters. Given a particular microwave background measurement, deciding on a particular set of parameters and various priors on those parameters is as much art as science. For the correct model, parameter values should be insensitive to the size of the parameter space or the particular priors invoked. Several particular parameter space analyses are mentioned below in Sec. 6.5.

## 6.2. Physical quantities

While the above parameters are useful and conventional for characterizing cosmological models, the features in the microwave background power spectrum depend on various physical quantities which can be expressed in terms of the parameters. Here the physical quantities are summarized, and their dependence on parameters given. This kind of analysis is important for understanding the model space of parameters as more than just a black box producing output power spectra. All of the physical dependences discussed here can be extracted from Hu and Sugiyama (1996). By comparing with numerical solutions to the evolution equations, Hu and Sugiyama demonstrated that they had accounted for all relevant physical processes.

Power-law initial conditions are determined in a straightforward way by the appropriate parameters  $Q$ ,  $n$ ,  $r$ , and  $n_T$ , if the perturbations are purely adiabatic. Additional parameters must be used to specify any departure from power law spectra, or to specify an additional admixture of isocurvature initial conditions (e.g. Bucher *et al.* 1999). These parameters directly express physical quantities.

On the other hand, the physical parameters determining the evolution of the initial perturbations until decoupling involve a few specific combinations of cosmological parameters. First, note that the density of radiation is fixed by the current microwave background temperature which is known from COBE, as well as the density of the neutrino backgrounds. The gravitational potentials describing scalar perturbations determine the size of the Sachs-Wolfe effect and also magnitude of the forces driving the acoustic oscillations. The potentials are determined by  $\Omega_0 h^2$ , the matter density as a fraction of critical density. The baryon density,  $\Omega_b h^2$ , determines the degree to which the acoustic peak amplitudes are modulated as described above in Sec. 5.4.

The time of matter-radiation equality is obviously determined solely by the total matter density  $\Omega_0 h^2$ . This quantity affects the size of the dark matter fluctuations, since dark matter starts to collapse gravitationally only after matter-radiation equality. Also, the gravitational potentials evolve in time during radiation domination and not during matter domination:

the later matter-radiation equality occurs, the greater the time evolution of the potentials at decoupling, increasing the Integrated Sachs-Wolfe effect. The power spectrum also has a weak dependence on  $\Omega_0$  in models with  $\Omega_0$  significantly less than unity, because at late times the evolution of the background cosmology will be dominated not by matter, but rather by vacuum energy (for a flat universe with  $\Lambda$ ) or by curvature (for an open universe). In either case, the gravitational potentials once again begin to evolve with time, giving an additional late-time Integrated Sachs-Wolfe contribution, but this tends to affect only the largest scales for which the constraints from measurements are least restrictive due to cosmic variance (see the discussion in Sec. 6.4 below).

The sound speed, which sets the sound horizon and thus affects the wavelength of the acoustic modes (cf. Eq. (28)), is completely determined by the baryon density  $\Omega_b h^2$ . The horizon size at recombination, which sets the overall scale of the acoustic oscillations, depends only on the total mass density  $\Omega_0 h^2$ . The damping scale for diffusion damping depends almost solely on the baryon density  $\Omega_b h^2$ , although numerical fits give a slight dependence on  $\Omega_b$  alone (Hu and Sugiyama 1996). Finally, the angular diameter distance to the surface of last scattering is determined by  $\Omega_0 h$  and  $\Lambda h$ ; the angular diameter sets the angular scale on the sky of the acoustic oscillations.

In summary, the physical dependence of the temperature perturbations at last scattering depends on  $\Omega_0 h^2$ ,  $\Omega_b h^2$ ,  $\Omega_0 h$ , and  $\Lambda h$  instead of the individual cosmological parameters  $\Omega_0$ ,  $\Omega_b$ ,  $h$ , and  $\Lambda$ . When analyzing constraints on cosmological models from microwave background power spectra, it may be more meaningful and powerful to constrain these physical parameters rather than the cosmological ones.

### 6.3. Power spectrum degeneracies

As might be expected from the above discussion, not all of the parameters considered here are independent. In fact, one nearly exact degeneracy exists if  $\Omega_0$ ,  $\Omega_b$ ,  $h$ , and  $\Lambda$  are taken as independent parameters. To see this, consider a shift in  $\Omega_0$ . In isolation, such a shift will produce a corresponding stretching of the power spectrum in  $l$ -space. But this effect can be compensated by first shifting  $h$  to keep  $\Omega_0 h^2$  constant, then shifting  $\Omega_b$  to keep  $\Omega_b h^2$  constant, and finally shifting  $\Lambda$  to keep the angular diameter distance constant. This set of shifted parameters will, in linear perturbation theory, produce almost exactly the same microwave background power spectra as the original set of parameters. The universe with shifted parameters will generally not be flat, but the resulting late-time Integrated Sachs-Wolfe effect only weakly break the degeneracy. Likewise, gravitational lensing has only a very weak effect on the degeneracy.

But all is not lost. The required shift in  $\Lambda$  is generally something like 8 times larger than the original shift in  $\Omega_0$ , so although the degeneracy is nearly exact, most of the degenerate models represent rather extreme cosmologies. Good taste requires either that  $\Lambda = 0$  or that  $\Omega = 1$ , in other words that we disfavor models which have both a cosmological constant and are not flat. If such models are disallowed, the degeneracy disappears. Finally, other observables not associated with the microwave background break the degeneracy: the acceleration parameter  $q_0 = \Omega_0/2 - \Lambda$ , for example, is measured directly by the high-redshift supernova experiments. So in practice, this fundamental degeneracy in the microwave background power spectrum between  $\Omega$  and  $\Lambda$  is not likely to have a great impact on our ability to constrain cosmological parameters.

Other approximate degeneracies in the temperature power spectrum exist between  $Q$  and  $r$ , and between  $z_r$  and  $n$ . The first is illusory: the amplitudes of the scalar and tensor power spectra can be used in place of their sum and ratio, which eliminates the degeneracy. The power spectrum of large-scale structure will lift the latter degeneracy if bias is understood well enough, as will polarization measurements and small-scale second-order temperature fluctuations (the Ostriker-Vishniac effect, see Jaffe and Gnedin 2000) which are both sensitive to  $z_r$ .

Finally, many claims have been made about the ability of the microwave background to constrain the effective number of neutrino species or neutrino masses. The effective number of massless degrees of freedom at decoupling can be expressed in terms of the effective number of neutrino species  $N_\nu$  (which does not need to be an integer). This is a convenient way of parameterizing ignorance about fundamental particle constituents of nature. Contributors to  $N_\nu$  could include, for example, an extra sterile neutrino sometimes invoked in neutrino oscillation models, or the thermal background of gravitons which would exist if inflation did not occur. This parameter can also include the effects of entropy increases due to decaying or annihilating particles; see Chapter 3 of Kolb and Turner (1990) for a detailed discussion. As far as the microwave background is concerned,  $N_\nu$  determines the radiation energy density of the universe and thus modifies the time of matter-radiation equality. It can in principle be distinguished from a change in  $\Omega_0 h^2$  because it affects other physical parameters like the baryon density or the angular diameter distance differently than a shift in either  $\Omega_0$  or  $h$ .

Neutrino masses cannot provide the bulk of the dark matter, because their free streaming greatly suppresses fluctuation power on galaxy scales, leading to a drastic mismatch with observed large-scale structure. But models with some small fraction of dark matter as neutrinos have been advocated to improve the agreement between the predicted and observed large-scale structure power spectrum. Massive neutrinos have several small effects on the microwave background, which have been studied systematically by Dodelson *et al.* (1996).

They can slightly increase the sound horizon at decoupling due to their transition from relativistic to non-relativistic behavior as the universe expands. More importantly, free streaming of massive neutrinos around the time of last scattering leads to a faster decay of the gravitational potentials, which in turn means more forcing of the acoustic oscillations and a resulting increase in the monopole perturbations. Finally, since matter-radiation equality is slightly delayed for neutrinos with cosmologically interesting masses of a few eV, the gravitational potentials are less constant and a larger Integrated Sachs-Wolfe effect is induced. The change in sound horizon and shift in matter-radiation equality due to massive neutrinos cannot be distinguished from changes in  $\Omega_b h^2$  and  $\Omega_0 h^2$ , but the alteration of the gravitational potential's time dependence due to neutrino free streaming cannot be mimicked by some other change in parameters. In principle the effect of neutrino masses can be extracted from the microwave background, although the effects are very small.

#### 6.4. Idealized experiments

Remarkably, the microwave background power spectrum contains enough information to constrain numerous parameters simultaneously (Jungman *et al.* 1996). We would like to estimate quantitatively just how well the space of parameters described above can be constrained by ideal measurements of the microwave background. The question has been studied in some detail; this section outlines the basic methods and results, and discusses how good various approximations are. For simplicity, only temperature fluctuations are considered in this section; the corresponding formalism for the polarization power spectra is developed in Kamionkowski *et al.* (1997).

Given a pixelized map of the microwave sky, we need to determine the contribution of pixelization noise, detector noise, and beam width to the multipole moments and power spectrum. Consider a temperature map of the sky  $T^{\text{map}}(\hat{\mathbf{n}})$  which is divided into  $N_{\text{pix}}$  equal-area pixels. The observed temperature in pixel  $j$  is due to a cosmological signal plus noise,  $T_j^{\text{map}} = T_j + T_j^{\text{noise}}$ . The multipole coefficients of the map can be constructed as

$$\begin{aligned} d_{lm}^{\Gamma} &= \frac{1}{T_0} \int d\hat{\mathbf{n}} T^{\text{map}}(\hat{\mathbf{n}}) Y_{lm}(\hat{\mathbf{n}}) \\ &\simeq \frac{1}{T_0} \sum_{j=1}^{N_{\text{pix}}} \frac{4\pi}{N_{\text{pix}}} T_j^{\text{map}} Y_{lm}(\hat{\mathbf{n}}_j), \end{aligned} \quad (31)$$

where  $\hat{\mathbf{n}}_j$  is the direction vector to pixel  $j$ . The map moments are written as  $d_{lm}$  to distinguish them from the moments of the cosmological signal  $a_{lm}$ ; the former include the effects of noise. The extent to which the second line in Eqs. (31) is only an approximate equality is

the pixelization noise. Most current experiments oversample the sky with respect to their beam, so the pixelization noise is negligible. Now assume that the noise is uncorrelated between pixels and is well-represented by a normal distribution. Also, assume that the map is created with a gaussian beam with width  $\theta_b$ . Then it is straightforward to show that the variance of the temperature moments is given by (Knox 1995)

$$\langle d_{lm}^T d_{l'm'}^{T*} \rangle = \left( C_l e^{-l^2 \sigma_b^2} + w^{-1} \right) \delta_{ll'} \delta_{mm'}, \quad (32)$$

where  $\sigma_b = 0.00742(\theta_b/1^\circ)$  and

$$w^{-1} = \frac{4\pi}{N_{\text{pix}}} \frac{\langle (T_i^{\text{noise}})^2 \rangle}{T_0^2} \quad (33)$$

is the inverse statistical weight per unit solid angle, a measure of experimental sensitivity independent of the pixel size.

Now the power spectrum can be estimated via Eq. (32) as

$$C_l^T = (D_l^T - w^{-1}) e^{l^2 \sigma_b^2} \quad (34)$$

where

$$D_l^T = \frac{1}{2l+1} \sum_{m=-l}^l d_{lm}^T d_{lm}^{T*}. \quad (35)$$

The individual coefficients  $d_{lm}^T$  are gaussian random variables. This means that  $C_l^T$  is a random variable with a  $\chi_{2l+1}^2$  distribution, and its variance is (Knox 1995)

$$(\Delta C_l^T)^2 = \frac{2}{2l+1} \left( C_l + w^{-1} e^{l^2 \sigma_b^2} \right). \quad (36)$$

Note that even for  $w^{-1} = 0$ , corresponding to zero noise, the variance is non-zero. This is the cosmic variance, arising from the fact that we have only one sky to observe: the estimator in Eq. (35) is the sum of  $2l+1$  random variables, so it has a fundamental fractional variance of  $(2l+1)^{-1/2}$  simply due to Poisson statistics. This variance provides a benchmark for experiments: if the goal is to determine a power spectrum, it makes no sense to improve resolution or sensitivity beyond the level at which cosmic variance is the dominant source of error.

Equation (36) is extremely useful: it gives an estimate of how well the power spectrum can be determined by an experiment with a given beam size and detector noise. If only a portion of the sky is covered, the variance estimate should be divided by the fraction of the total sky covered. With these variances in hand, standard statistical techniques

can be employed to estimate how well a given measurement can recover a given set  $\mathbf{s}$  of cosmological parameters. Approximate the dependence of  $C_l^T$  on a given parameter as linear in the parameter; this will always be true for some sufficiently small range of parameter values. Then the parameter space curvature matrix (also known as the Fisher information matrix) is specified by

$$\alpha_{ij} = \sum_l \frac{\partial C_l^T}{\partial s_i} \frac{\partial C_l^T}{\partial s_j} \frac{1}{(\Delta C_l^T)^2}. \quad (37)$$

The variance in the determination of the parameter  $s_i$  from a set of  $C_l^T$  with variances  $\Delta C_l^T$  after marginalizing over all other parameters is given by the diagonal element  $i$  of the matrix  $\alpha^{-1}$ .

Estimates of this kind were first made by Jungman *et al.* (1996) and subsequently refined by Zaldarriaga *et al.* (1998) and Bond *et al.* (1998), among others. The basic result is that a map with pixels of a few arcminutes in size and a signal-to-noise ratio of around 1 per pixel can determine  $\Omega$ ,  $\Omega_b h^2$ ,  $\Omega_m h^2$ ,  $\Lambda h^2$ ,  $Q$ ,  $n$ , and  $z_r$  at the few percent level *simultaneously*, up to the one degeneracy mentioned above (see the table in Bond *et al.* 1998). Significant constraints will also be placed on  $r$  and  $N_\nu$ . This prospect has been the primary reason that the microwave background has generated such excitement. Note that  $\Omega$ ,  $h$ ,  $\Omega_b$ , and  $\Lambda$  are the classical cosmological parameters. Decades of painstaking astronomical observations have been devoted to determining the values of these parameters. The microwave background offers a completely independent method of determining them with comparable or significantly greater accuracy, and with fewer astrophysical systematic effects to worry about. The microwave background is also the only source of precise information about the spectrum and character of the primordial perturbations from which we arose. Of course, these exciting possibilities hold only if the universe is accurately represented by a model in the assumed model space. The model space is, however, quite broad. Model-independent constraints which the microwave background provides are discussed in Sec. 7.

The estimates of parameter variances based on the curvature matrix would be exact if the power spectrum always varied linearly with each parameter. This, of course, is not true in general. Given a set of power spectrum data, we want to know two pieces of information about the cosmological parameters: (1) What parameter values provide the best-fit model? (2) What are the error bars on these parameters, or more precisely, what is the region of parameter space which defines a given confidence level? The first question can be answered easily using standard methods of searching parameter space; generally such a search requires evaluating the power spectrum for fewer than 100 different models. This shows that the parameter space is generally without complicated structure or many false minima. The second question is more difficult. Anything beyond the curvature matrix analysis requires looking around in parameter space near the best-fit model. A specific Monte Carlo technique em-

ploying a Metropolis algorithm has recently been advocated (Christensen and Meyer 2000); such techniques will certainly prove more flexible and efficient than recent brute-force grid searches (Tegmark and Zaldarriaga 2000). As upcoming data sets contain more information and consequently have greater power to constrain parameters, efficient techniques of parameter space exploration will become increasingly important.

To this point, the discussion has assumed that the microwave background power spectrum is perfectly described by linear perturbation theory. Since the temperature fluctuations are so small, parts in a hundred thousand, linear theory is a very good approximation. However, on small scales, non-linear effects become important and can dominate over the linear contributions. The most important non-linear effects are the Ostriker-Vishniac effect coupling velocity and density perturbations (Jaffe and Kamionkowski 1998, Hu 2000), gravitational lensing by large-scale structure (Seljak 1996), the Sunyaev-Zeldovich effect which gives spectral distortions when the microwave background radiation passes through hot ionized regions (Birkinshaw 1999), and the kinetic Sunyaev-Zeldovich effect which doppler shifts radiation passing through plasma with bulk velocity (Gnedin and Jaffe 2000). All three effects are measurable and give important additional constraints on cosmology, but more detailed descriptions are outside the scope of these lectures.

Finally, no discussion of parameter determination would be complete without mention of galactic foreground sources of microwave emission. Dust radiates significantly at microwave frequencies, as do free-free and synchrotron emission; point source microwave emission is also a potential problem. Dust emission generally has a spectrum which rises with frequency, while free-free and synchrotron emission have falling frequency spectra. The emission is not uniform on the sky, but rather concentrated in the galactic plane, with fainter but pervasive diffuse emission in other parts of the sky. The dust and synchrotron/free-free emission spectra cross each other at a frequency of around 90 GHz. Fortunately for cosmologists, the amplitude of the foreground emission at this frequency is low enough to create a frequency window in which the cosmological temperature fluctuations dominate the foreground temperature fluctuations. At other frequencies, the foreground contribution can be effectively separated from the cosmological blackbody signal by measuring in several different frequencies and projecting out the portion of the signal with a flat frequency spectrum. The foreground situation for polarization is less clear, both in amplitude and spectral index, and could potentially be a serious systematic limit to the quality of cosmological polarization data. On the other hand, it may be no greater problem for polarization fluctuations than for temperature fluctuations. For an overview of issues surrounding foreground emission, see Bouchet and Gispert 1999 or the WOMBAT web site, <http://astro.berkeley.edu/wombat>.

### 6.5. Current constraints and upcoming experiments

As the Como School began, results from the high-resolution balloon-born experiment MAXIMA (Hanany *et al.* 2000) were released, complementing the week-old data from BOOMERanG (de Bernardis *et al.* 2000) and creating a considerable buzz at coffee breaks. The derived power spectrum estimates are shown in Fig. 3. The data from the two measurements appear consistent up to calibration uncertainties, and for simplicity will be referred to here as “balloon data” and discussed as a single result. While a few experimenters and data analyzers were members of both experimental teams, the measurements and data reductions were done essentially independently. Earlier data from the previous year (Miller *et al.* 1999) had clearly demonstrated the existence and angular scale of the first peak in the power spectrum and produced the first maps of the microwave background at angular scales below a degree. But the new results from balloon experiments utilizing extremely sensitive bolometric detectors represent a qualitative step forward. These experiments begin to exploit the potential of the microwave background for “precision cosmology”; their power spectra put strong constraints on several cosmological parameters simultaneously and rule out many variants of cosmological models. In fact, what is most interesting is that, at face value, these measurements put significant pressure on all of the standard models outlined above.

The balloon data shows two major features: first, a large peak in the power spectrum centered around  $l = 200$  with an amplitude of approximately  $l^2 C_l = 36000 \mu\text{K}^2$ , and second, a broad plateau between  $l = 400$  and  $l = 700$  with an amplitude of approximately  $l^2 C_l = 10000 \mu\text{K}^2$ . The first peak is clearly delineated and provides good evidence that the universe is spatially flat, i.e.  $\Omega = 1$ . The issue of a second acoustic peak is much less clear. In most flat universe models with acoustic oscillations, the second peak is expected to appear at an angular scale of around  $l = 400$ . The angular resolution of the balloon experiments is certainly good enough to see such a peak, but the power spectrum data shows no evidence for one. I argue that a flat line is an excellent fit to the data past  $l = 300$ , and that any model which shows a peak in this region will be a worse fit than a flat line. This does not necessarily mean that no peak is present; the error bars are too large to rule out a peak, but the amplitude of such a peak is fairly strongly constrained to be lower than expected given the first peak.

What does this mean for cosmological models? Within the model space outlined in the previous section, there are three ways to suppress the second peak. The first would be to have a power spectrum index  $n$  substantially less than 1. This solution would force abandonment of the assumption of power law initial fluctuations, in order to match the observed amplitude of large-scale structure at smaller scales. While this is certainly possible, it

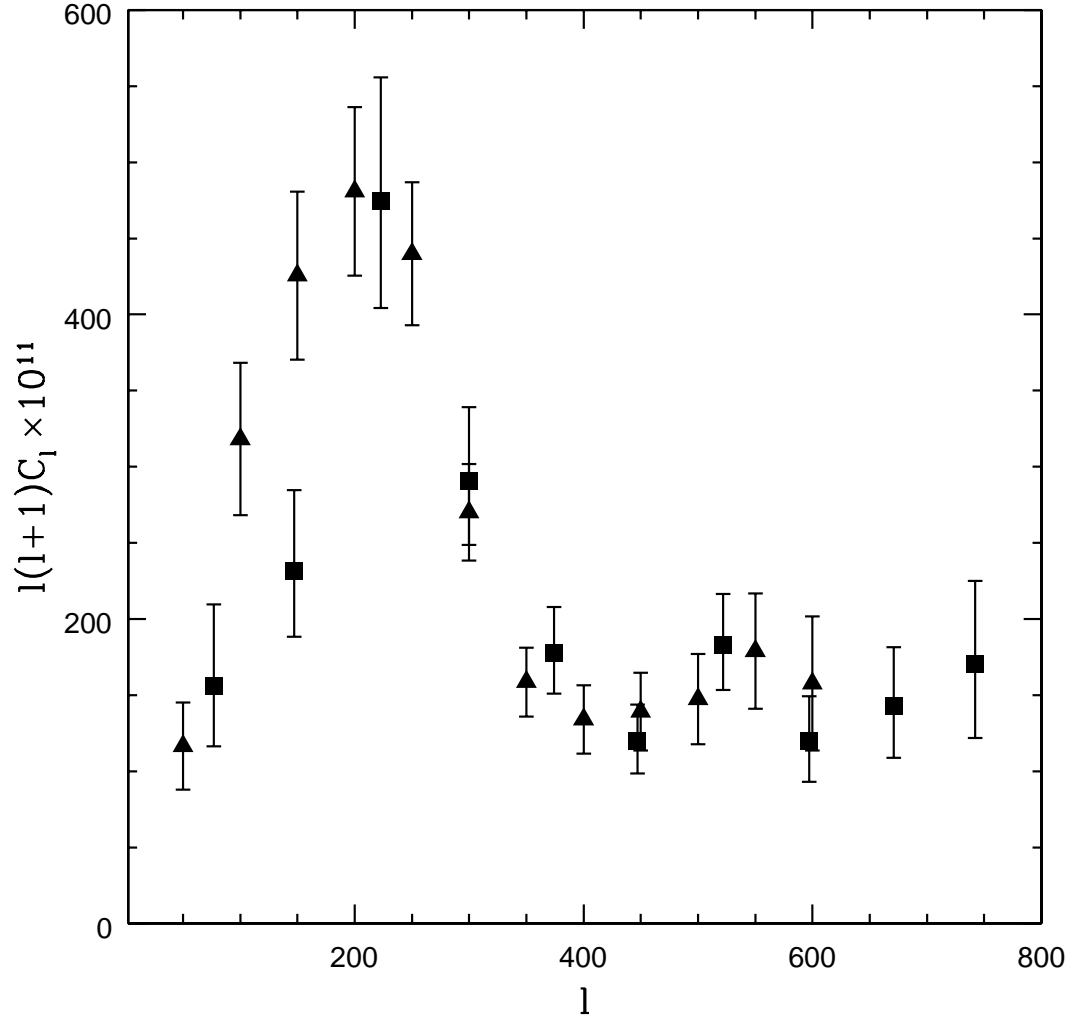


Fig. 3.— Two current measurements of the microwave background radiation temperature power spectrum. Triangles are BOOMERanG measurements multiplied by 1.21; squares are MAXIMA measurements multiplied by 0.92. The normalization factors are within the calibration uncertainties of the experiments, and were chosen by Hanany et al. (2000) to give the most consistent results between the two experiments.

represents a drastic weakening in the predictive power of the microwave background: essentially, a certain feature is reproduced by arbitrarily changing the primordial power spectrum. While no physical principle requires power law primordial perturbations, we should wait for microwave background measurements on a much wider range of scales combined with overlapping large-scale structure measurements before resorting to departures from power-law initial conditions. If the universe really did possess an initial power spectrum with a variety of features in it, most of the promise of precision cosmology is lost. Recent power spectra extracted from the IRAS Point Source Survey Redshift Catalog (Tegmark and Hamilton 2000), which show a remarkable power law behavior spanning three orders of magnitude in wave number, seem to argue against this possibility.

The second possibility is a drastic amount of reionization. It is not clear the extent to which this might be compatible with the height of the first peak and still suppress the second peak sufficiently. This possibility seems unlikely as well, but would show clear signatures in the microwave background polarization.

The most commonly discussed possibility is that the very low second peak amplitude reflects an unexpectedly large fraction of baryons relative to dark matter in the universe. The baryon signature discussed in Sec. 5.4 gives a suppression of the second peak in this case. However, primordial nucleosynthesis also constrains the baryon-photon ratio. Recent high-precision measurements of deuterium absorption in high-redshift neutral hydrogen clouds (Tytler *et al.* 2000) give a baryon-photon number ratio of  $\eta = 5.1 \pm 0.5 \times 10^{10}$ , which translates to  $\Omega_b h^2 = 0.019 \pm 0.002$  assuming that the entropy (i.e. photon number) per comoving volume remains constant between nucleosynthesis and the present. Requiring  $\Omega_b$  to satisfy this nucleosynthesis constraint leads to microwave background power spectra which are not particularly good fits to the data. An alternative is that the entropy per comoving volume has *not* remained fixed between nucleosynthesis and recombination (see, e.g., Kaplinghat and Turner 2000). This could be arranged by having a dark matter particle which decays to photons, although such a process must evade limits from the lack of microwave background spectral distortions (Hu and Silk 1993). Alternately, a large chemical potential for the neutrino background could lead to larger inferred values for the baryon-photon ratio from nucleosynthesis (Esposito *et al.* 2000). Either way, if both the microwave background measurements and the high-redshift deuterium abundances hold up, the discrepancy points to new physics. Of course, a final explanation for the discrepancies is simply that the balloon data has significant systematic errors.

I digress for a brief editorial comment about data analysis. Straightforward searches of the conventional cosmological model space described above for good fits to the balloon data give models with very low dark matter densities, high baryon fractions, and very large

cosmological constants (see model P1 in Table 1 of Lange *et al.* 2000). Such models violate other observational constraints on age, which must be at least 12 billion years (see, e.g., Peacock *et al.* 1998), and quasar and radio source strong lensing number counts, which limit a cosmological constant to  $\Lambda \leq 0.7$  (Falco *et al.* 1998). The response to this situation so far has been to invoke Bayesian prior probability distributions on various quantities like  $\Omega_b$  and the age. This leads to a best-fit model with a nominally acceptable  $\chi^2$  (Lange *et al.* 2000, Tegmark *et al.* 2000 and others). But be wary of this procedure when the priors have a large effect on the best-fit model! The microwave background will soon provide tighter constraints on most parameters than any other source of prior information. Priors probabilities on a given parameter are useful and justified when the microwave background data has little power to constrain that parameter; in this case, the statistical quality of the model fit to the microwave background data will not be greatly affected by imposing the prior. However, something fishy is probably going on when a prior pulls a parameter multiple sigma away from its best fit value without the prior. This is what happens presently with  $\Omega_b$  when the nucleosynthesis prior is enforced. If your priors make a big difference, it is likely either that some of the data is incorrect, or that the model space does not include the correct model. Both the microwave background measurements and the high-redshift deuterium detections are taxing observations dominated by systematic effects, so it is certainly possible that one or both are wrong. On the other hand, MAXIMA and BOOMERanG are consistent with each other while using different instruments, different parts of the sky, and different analysis pipelines, and the deuterium measurements are consistent for several different clouds. This suggests possible missing physics ingredients, like extreme reionization or an entropy increase mentioned above, or perhaps significant contributions from cosmic defects. It has even been suggested by otherwise sober and reasonable people that the microwave background results, combined with various difficulties related to dynamics of spiral galaxies, may point towards a radical revision of the standard cosmology (Sellwood and Kosowsky 2000). We should not rest lightly until the cosmological model preferred by microwave background measurements is comfortably consistent with all relevant priors derived from other data sources of comparable precision.

The picture will come into sharper relief over the next two years. The MAP satellite (<http://map.gsfc.nasa.gov>), due for launch by NASA in May, 2001, will map the full microwave sky in five frequency channels with an angular resolution of around 15 arc minutes and a temperature sensitivity per pixel of a part in a million. Space missions offer unequalled sky coverage and control of systematics, and if it works as advertised, MAP will be a benchmark experiment. Prior to its launch, expect to see the first interferometric microwave data at angular scales smaller than a half degree from the CBI interferometer experiment (<http://www.astro.caltech.edu/~tjp/CBI/>). In this same time frame, we also

may have the first detection of polarization. The most interesting power spectrum feature to focus on will be the existence and amplitude of a third acoustic peak. If a third peak appears with amplitude significantly higher than the putative second peak, this almost certainly indicates conventional acoustic oscillations with a high baryon fraction and possibly new physics to reconcile the result with the deuterium measurements. If, on the other hand, the power spectrum remains flat or falls further past the second peak region, then all bets are off. In a time frame of the next 5 to 10 years, we can reasonably expect to have a cosmic-variance limited temperature power spectrum down to scales of a few arcminutes (say,  $l = 4000$ ), along with significant polarization information (though probably not cosmic-variance limited power spectra). In particular, ESA's Planck satellite mission (<http://astro.estec.esa.nl/SA-general/Projects/Planck/>) will map the microwave sky in nine frequency bands at significantly better resolution and sensitivity than the MAP mission. For a comprehensive listing of past and planned microwave background measurements, see Max Tegmark's experiments web page, <http://www.hep.upenn.edu/~max/cmb/experiments.html>.

## 7. Model-Independent Cosmological Constraints

Most analysis of microwave background data and predictions about its ability to constrain cosmology have been based on the cosmological parameter space described in Sec. 6.1 above. This space is motivated by inflationary cosmological scenarios, which generically predict power-law adiabatic perturbations evolving only via gravitational instability. Considering that this space of models is broad and appears to fit all current data far better than any other proposed models, such an assumed model space is not very restrictive. In particular, proposed extensions tend to be rather ad hoc, adding extra elements to the model without providing any compelling underlying motivation for them. Examples which have been discussed in the literature include multiple types of dark matter with various properties, nonstandard recombination, small admixtures of topological defects, production of excess entropy, or arbitrary initial power spectra. None of these possibilities are attractive from an aesthetic point of view: all add significant complexity and freedom to the models without any corresponding restrictions on the original parameter space. The principle of Occam's Razor should cause us to be skeptical about any such additions to the space of models.

On the other hand, it is possible that some element *is* missing from the model space, or that the actual cosmological model is radically different in some respect. The microwave background is the probe of cosmology most tightly connected to the fundamental properties

of the universe and least influenced by astrophysical complications, and thus the most capable data source for deciding whether the universe actually is well described by some model in the usual model space. An interesting question is the extent to which the microwave background can determine various properties of the universe independent from particular models. While any cosmological interpretation of temperature fluctuations in the microwave sky requires some kind of minimal assumptions, all of the conclusions outlined below can be drawn without invoking a detailed model of initial conditions or structure formation. These conclusions are in contrast to precision determination of cosmological parameters, which does require the assumption of a particular space of models and which can vary significantly depending on the space.

### 7.1. Flatness

The Friedmann-Robertson-Walker spacetime describing homogeneous and isotropic cosmology comes in three flavors of spatial curvature: positive, negative, and flat, corresponding to  $\Omega > 1$ ,  $\Omega < 1$ , and  $\Omega = 1$  respectively. One of the most fundamental questions of cosmology, dating to the original relativistic cosmological models, is the curvature of the background spacetime. The fate of the universe quite literally depends on the answer: in a cosmology with only matter and radiation, a positively-curved universe will eventually recollapse in a fiery “Big Crunch” while flat and negatively-curved universes will expand forever, meeting a frigid demise. Note these fates are at least 40 billion years in the future. (A cosmological constant or other energy density component with an unusual equation of state can alter these outcomes, causing a closed universe eventually to enter an inflationary stage.)

The microwave background provides the cleanest and most powerful probe of the geometry of the universe (Kamionkowski *et al.* 1994). The surface of last scattering is at a high enough redshift that photon geodesics between the last scattering surface and the Earth are significantly curved if the geometry of the universe is appreciably different than flat. In a positively-curved space, two geodesics will bend towards each other, subtending a larger angle at the observer than in the flat case; likewise, in a negatively-curved space two geodesics bend away from each other, resulting in a smaller observed angle between the two. The operative quantity is the angular diameter distance; Weinberg (2000) gives a pedagogical discussion of its dependence on  $\Omega$ . In a flat universe, the horizon length at the time of last scattering subtends an angle on the sky of around two degrees. For a low-density universe with  $\Omega = 0.3$ , this angle becomes smaller by half, roughly.

A change in angular scale of this magnitude will change the apparent scale of all physical scales in the microwave background. A model-independent determination of  $\Omega$  thus requires

a physical scale of known size to be imprinted on the primordial plasma at last scattering; this physical scale can then be compared with its apparent observed scale to obtain a measurement of  $\Omega$ . The microwave background fluctuations actually depend on two basic physical scales. The first is the sound horizon at last scattering,  $r_s$  (cf. Eq. (29)). If coherent acoustic oscillations are visible, this scale sets their characteristic wavelengths. Even if coherent acoustic oscillations are not present, the sound horizon represents the largest scale on which any causal physical process can influence the primordial plasma. Roughly, if primordial perturbations appear on all scales, the resulting microwave background fluctuations appear as a featureless power law at large scales, while the scale at which they begin to depart from this assumed primordial behavior corresponds to the sound horizon. This is precisely the behavior observed by current measurements, which show a prominent power spectrum peak at an angular scale of a degree ( $l = 200$ ), arguing strongly for a flat universe. Of course, it is logically possible that the primordial power spectrum has power on scales only significantly smaller than the horizon at last scattering. In this case, the largest scale perturbations would appear at smaller angular scales for a given geometry. But then the observed power-law perturbations at large angular scales must be reproduced by the Integrated Sachs-Wolfe effect, and resulting models are contrived. If the microwave background power spectrum exhibits acoustic oscillations, then the spacing of the acoustic peaks depends only on the sound horizon independent of the phase of the oscillations; this provides a more general and precise probe of flatness than the first peak position.

The second physical scale provides another test: the Silk damping scale is determined solely by the thickness of the surface of last scattering, which in turn depends only on the baryon density  $\Omega_b h^2$ , the expansion rate of the universe and standard thermodynamics. Observation of an exponential suppression of power at small scales gives an estimate of the angular scale corresponding to the damping scale. Note that the effects of reionization and gravitational lensing must both be accounted for in the small-scale dependence of the fluctuations. If the reionization redshift can be accurately estimated from microwave background polarization (see below) and the baryon density is known from primordial nucleosynthesis or from the alternating peak heights signature (Sec. 5.4), only a radical modification of the standard cosmology altering the time dependence of the scale factor or modifying thermodynamic recombination can change the physical damping scale. If the estimates of  $\Omega$  based on the sound horizon and damping scales are consistent, this is a strong indication that the inferred geometry of the universe is correct.

## 7.2. Coherent acoustic oscillations

If a series of peaks equally spaced in  $l$  is observed in the microwave background temperature power spectrum, it strongly suggests we are seeing the effects of coherent acoustic oscillations at the time of last scattering. Microwave background polarization provides a method for confirming this hypothesis. As explained in Sec. 4.2, polarization anisotropies couple primarily to velocity perturbations, while temperature anisotropies couple primarily to density perturbations. Now coherent acoustic oscillations produce temperature power spectrum peaks at scales where a mode of that wavelength has either maximum or minimum compression in potential wells at the time of last scattering. The fluid velocity for the mode at these times will be zero, as the oscillation is turning around from expansion to contraction (envision a mass on a spring.) At scales intermediate between the peaks, the oscillating mode has zero density contrast but a maximum velocity perturbation. Since the polarization power spectrum is dominated by the velocity perturbations, its peaks will be at scales interleaved with the temperature power spectrum peaks. This alternation of temperature and polarization peaks as the angular scale changes is characteristic of acoustic oscillations (see Kosowsky (1999) for a more detailed discussion). Indeed, it is almost like seeing the oscillations directly: it is difficult to imagine any other explanation for density and velocity extrema on alternating scales. The temperature-polarization cross-correlation must also have peaks with corresponding phases. This test will be very useful if a series of peaks is detected in a temperature power spectrum which is not a good fit to the standard space of cosmological models. If the peaks turn out to reflect coherent oscillations, we must then modify some aspect of the underlying cosmology, while if the peaks are not coherent oscillations, we must modify the process by which perturbations evolve.

If coherent oscillations are detected, any cosmological model must include a mechanism for enforcing coherence. Perturbations on all scales, in particular on scales outside the horizon, provide the only natural mechanism: the phase of the oscillations is determined by the time when the wavelength of the perturbation becomes smaller than the horizon, and this will clearly be the same for all perturbations of a given wavelength. For any source of perturbations inside the horizon, the source itself must be coherent over a given scale to produce phase-coherent perturbations on that scale. This cannot occur without artificial fine-tuning.

## 7.3. Adiabatic primordial perturbations

If the microwave background temperature and polarization power spectra reveal coherent acoustic oscillations and the geometry of the universe can also be determined with some

precision, then the phases of the acoustic oscillations can be used to determine whether the primordial perturbations are adiabatic or isocurvature. Quite generally, Eq. (28) shows that adiabatic and isocurvature power spectra must have peaks which are out of phase. While current measurements of the microwave background and large-scale structure rule out models based entirely on isocurvature perturbations, some relatively small admixture of isocurvature modes with dominant adiabatic modes is possible. Such mixtures arise naturally in inflationary models with more than one dynamical field during inflation (see, e.g., Mukhanov and Steinhardt 1998).

#### 7.4. Gaussian primordial perturbations

If the temperature perturbations are well approximated as a gaussian random field, as microwave background maps so far suggest, then the power spectrum  $C_l$  contains all statistical information about the temperature distribution. Departures from gaussianity take myriad different forms; the business of providing general but useful statistical descriptions is a complicated one (see, e.g., Ferreira *et al.* 1997). Tiny amounts of nongaussianity will arise inevitably from non-linear evolution of fluctuations, and larger nongaussian contributions can be a feature of the primordial perturbations or can be induced by “stiff” stress-energy perturbations such as topological defects. As explained below, defect theories of structure formation seem to be ruled out by current microwave background and large-scale structure measurements, so interest in nongaussianity has waned. But the extent to which the temperature fluctuations are actually gaussian is experimentally answerable, and as observations improve this will become an important test of inflationary cosmological models.

#### 7.5. Tensor or vector perturbations

As described in Sec. 4.3, the tensor field describing microwave background polarization can be decomposed into two components corresponding to the gradient-curl decomposition of a vector field. This decomposition has the same physical meaning as that for a vector field. In particular, any gradient-type tensor field, composed of the G-harmonics, has no curl, and thus may not have any handedness associated with it (meaning the field is even under parity reversal), while the curl-type tensor field, composed of the C-harmonics, does have a handedness (odd under parity reversal).

This geometric interpretation leads to an important physical conclusion. Consider a universe containing only scalar perturbations, and imagine a single Fourier mode of the

perturbations. The mode has only one direction associated with it, defined by the Fourier vector  $\mathbf{k}$ ; since the perturbation is scalar, it must be rotationally symmetric around this axis. (If it were not, the gradient of the perturbation would define an independent physical direction, which would violate the assumption of a scalar perturbation.) Such a mode can have no physical handedness associated with it, and as a result, the polarization pattern it induces in the microwave background couples only to the G harmonics. Another way of stating this conclusion is that primordial density perturbations produce *no* C-type polarization as long as the perturbations evolve linearly. On the other hand, primordial tensor or vector perturbations produce both G-type and C-type polarization of the microwave background (provided that the tensor or vector perturbations themselves have no intrinsic net polarization associated with them).

Measurements of cosmological C-polarization in the microwave background are free of contributions from the dominant scalar density perturbations and thus can reveal the contribution of tensor modes in detail. For roughly scale-invariant tensor perturbations, most of the contribution comes at angular scales larger than  $2^\circ$  ( $2 < l < 100$ ). Figure 4 displays the C and G power spectra for scale-invariant tensor perturbations contributing 10% of the COBE signal on large scales. A microwave background map with foreseeable sensitivity could measure gravitational wave perturbations with amplitudes smaller than  $10^{-3}$  times the amplitude of density perturbations (Kamionkowski and Kosowsky 1998). The C-polarization signal also appears to be the best hope for measuring the spectral index  $n_T$  of the tensor perturbations.

## 7.6. Reionization redshift

Reionization produces a distinctive microwave background signature. It suppresses temperature fluctuations by increasing the effective damping scale, while it also increases large-angle polarization due to additional Thomson scattering at low redshifts when the radiation quadrupole fluctuations are much larger. This enhanced polarization peak at large angles will be significant for reionization prior to  $z = 10$  (Zaldarriaga 1997). Reionization will also greatly enhance the Ostriker-Vishniac effect, a second-order coupling between density and velocity perturbations (Jaffe and Kamionkowski 1998). The nonuniform reionization inevitable if the ionizing photons come from point sources, as seems likely, may also create an additional feature at small angular scales (Hu and Gruzinov 1998, Knox *et al.* 1998). Taken together, these features are clear indicators of the reionization redshift  $z_r$  independent of any cosmological model.

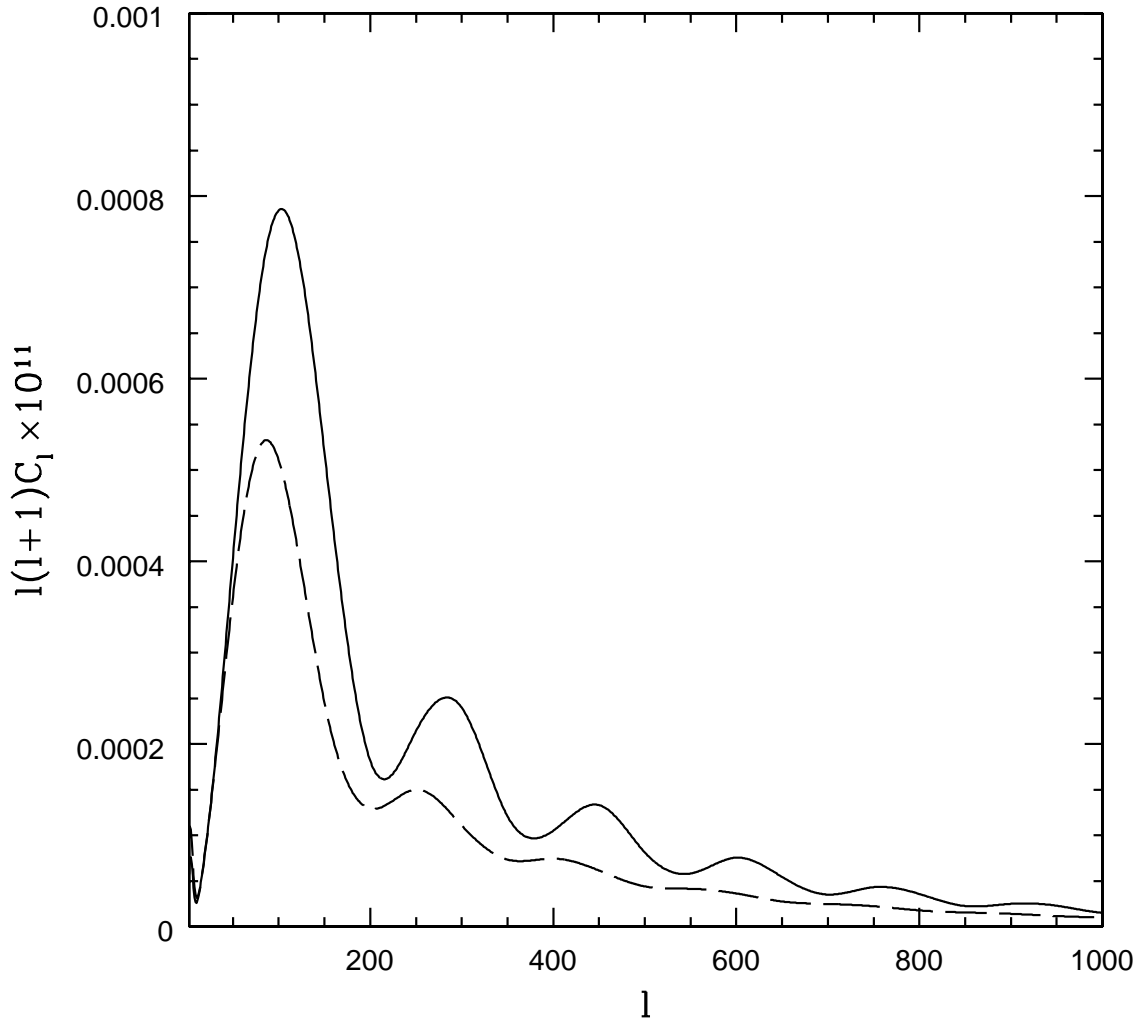


Fig. 4.— Polarization power spectra from tensor perturbations: the solid line is  $C_l^G$  and the dashed line is  $C_l^C$ . The amplitude gives a 10% contribution to the COBE temperature power spectrum measurement at low  $l$ . Note that scalar perturbations give no contribution to  $C_l^C$ .

## 7.7. Magnetic Fields

Primordial magnetic fields would be clearly indicated if cosmological Faraday rotation were detected in the microwave background polarization. A field with comoving field strength of  $10^{-9}$  gauss would produce a signal with a few degrees of rotation at 30 GHz, which is likely just detectable with future polarization experiments (Kosowsky and Loeb 1996). Faraday rotation has the effect of mixing G-type and C-type polarization, and would be another contributor to the C-polarization signal, along with tensor perturbations. Depolarization will also result from Faraday rotation in the case of significant rotation through the last scattering surface (Harari *et al.* 1996) Additionally, the tensor and vector metric perturbations produced by magnetic fields result in further microwave background fluctuations. A distinctive signature of such fields is that for a range of power spectra, the polarization fluctuations from the metric perturbations is comparable to, or larger than, the corresponding temperature fluctuations (Kahniashvili *et al.* 2000). Since the microwave background power spectra vary as the fourth power of the magnetic field amplitude, it is unlikely that we can detect magnetic fields with comoving amplitudes significantly below  $10^{-9}$  gauss. However, if such fields do exist, the microwave background provides several correlated signatures which will clearly reveal them.

## 7.8. The topology of the universe

Finally, one other microwave background signature of a very different character deserves mention. Most cosmological analyses make the implicit assumption that the spatial extent of the universe is infinite, or in practical terms at least much larger than our current Hubble volume so that we have no way of detecting the bounds of the universe. However, this need not be the case. The requirement that the unperturbed universe be homogeneous and isotropic determines the spacetime metric to be of the standard Friedmann-Robertson-Walker form, but this is only a *local* condition on the spacetime. Its global structure is still unspecified. It is possible to construct spacetimes which at every point have the usual homogeneous and isotropic metric, but which are spatially compact (have finite volumes). The most familiar example is the construction of a three-torus from a cubical piece of the flat spacetime by identifying opposite sides. Classifying the possible topological spaces which locally have the metric structure of the usual cosmological spacetimes (i.e. have the Friedmann-Robertson-Walker spacetimes as a topological covering space) has been studied extensively. The zero-curvature and positive-curvature cases have only a handful of possible topological spaces associated with them, while the negative curvature case has an infinite number with a very rich classification. See Weeks (1998) for a review.

If the topology of the universe is non-trivial and the volume of the universe is smaller than the volume contained by a sphere with radius equal to the distance to the surface of last scattering, then it is possible to detect the topology. Cornish *et al.* (1996) pointed out that because the last scattering surface is always a sphere in the covering space, any small topology will result in matched circles of temperature on the microwave sky. The two circles represent photons originating from the same physical location in the universe but propagating to us in two different directions. Of course, the temperatures around the circles will not match exactly, but only the contributions coming from the Sachs-Wolfe effect and the intrinsic temperature fluctuations will be the same; the velocity and Integrated Sachs-Wolfe contributions will differ and constitute a noise source. Estimates show the circles can be found efficiently via a direct search of full-sky microwave background maps. Once all matching pairs of circles have been discovered, their number and relative locations on the sky strongly overdetermine the topology of the universe in most cases. Remarkably, the microwave background essentially allows us to determine the size of the universe if it is smaller than the current horizon volume in any dimension.

## 8. Finale: Testing Inflationary Cosmology

In summary, the cosmic microwave background radiation is a remarkably interesting and powerful source of information about cosmology. It provides an image of the universe at an early time when the relevant physical processes were all very simple, so the dependence of anisotropies on the cosmological model can be calculated with high precision. At the same time, the universe at decoupling was an interesting enough place that small differences in cosmology will produce measurable differences in the anisotropies.

The microwave background has the ultimate potential to determine fundamental cosmological parameters describing the universe with percent-level precision. If this promise is realized, the standard model of cosmology would compare with the standard model of particle physics in terms of physical scope, explanatory power, and detail of confirmation. But in order for such a situation to come about, we must first choose a model space which includes the correct model for the universe. The accuracy with which cosmological parameters can be determined is of course limited by the accuracy with which some model in the model space represents the actual universe.

The space of models discussed in Sec. 6.1 represents universes which we would expect to arise from the mechanism of inflation. These models have become the standard testing ground for comparisons with data because they are simple, general, and well-motivated. So far, these types of models fit the data well, much better than any competing theories.

Future measurements may remain perfectly consistent with inflationary models, may reveal inconsistencies which can be remedied via minor extensions or modifications of the parameter space, or may require more serious departures from these types of models.

For the sake of a concluding discussion about the power of the microwave background, assume that the universe actually is well described by inflationary cosmology, and that it can be modelled by the parameters in Sec. 6.1. For an overview of inflation and the problems it solves, see Kolb and Turner (1990, chapter 8) or the lectures of A. Linde in this volume. To what extent can we hope to verify inflation, a process which likely would have occurred at an energy scale of  $10^{16}$  GeV when the universe was  $10^{-38}$  seconds old? Direct tests of physics at these energy scales are unimaginable, leaving cosmology as the only likely way to probe this physics.

Inflation is not a precise theory, but rather a mechanism for exponential expansion of the universe which can be realized in a variety of specific physical models. Cosmology in general and the cosmic microwave background in particular can hope to test the following predictions of inflation (see Kamionkowski and Kosowsky 1999 for a more complete discussion of inflation and its observable microwave background properties):

- The most basic prediction of inflation is a spatially flat universe. The flatness problem was one of the fundamental motivations for considering inflation in the first place. While it is possible to construct models of inflation which result in a non-flat universe, they all must be finely tuned for inflation to end at just the right time for a tiny but non-negligible amount of curvature to remain. The geometry of the universe is one of the fundamental pieces of physics which can be extracted from the microwave background power spectra. Recent measurements make a strong case that the universe is indeed flat.
- Inflation generically predicts primordial perturbations which have a gaussian statistical distribution. The microwave background is the only precision test of this prediction. Primordial gaussian perturbations will still be almost precisely gaussian at recombination, whereas they will have evolved significant nongaussianity by the time the local large-scale structure forms, due to gravitational collapse. Other methods of probing gaussianity, like number densities of galaxies or other objects, inevitably depend significantly on astrophysical modelling.
- The simplest models of inflation, with a single dynamical scalar field, give adiabatic primordial perturbations. The only real test of this prediction comes from the microwave background power spectrum. More complex models of inflation with multiple

dynamical fields generically result in dominant adiabatic fluctuations with some admixture of isocurvature fluctuations. Limits on isocurvature fluctuations obtained from microwave background measurements could be used to place constraints on the size of couplings between different fields at inflationary energy scales.

- Inflation generically predicts primordial perturbations on all scales, including scales outside the horizon. Of course we can never test directly whether perturbations on scales larger than the horizon exist, but the microwave background can reveal perturbations at recombination on scales comparable to the horizon scale. Zaldarriaga and Spergel (1997) have argued that inflation generically gives a peak in the polarization power spectrum at angular scales larger than  $2^\circ$ , and that no causal perturbations at the epoch of last scattering can produce a feature at such large scales. Inflation further predicts that the primordial power spectrum should be close to a scale-invariant power law (e.g. Huterer and Turner 2000), although complicated models can lead to power spectra with features or significant departures from scale invariance. The microwave background can probe the primordial power spectrum over three orders of magnitude.
- Inflationary perturbations result in phase-coherent acoustic oscillations. The coherence arises because on any given scale, the perturbations start in the same state determined only by their character outside the horizon. For a discussion in the language of squeezed quantum states, see Albrecht (2000). It is extremely difficult to produce coherent oscillations by any mechanism other than perturbations outside the horizon. The microwave background temperature and polarization power spectra will together clearly reveal coherent oscillations.
- Inflation finally predicts potentially measurable relationships between the amplitudes and power law indices of the primordial density and gravitational wave perturbations (see Lidsey *et al.* 1997 for a comprehensive overview), and measuring a  $C_l^C$  power spectrum appears to be the only way to obtain precise enough measurements of the tensor perturbations to test these predictions, thanks to the fact that the density perturbations don't contribute to  $C_l^C$ . Detection of inflationary tensor perturbations would reveal the energy scale at which inflation occurred, while confirming the inflationary relationships between scalar and tensor perturbations would provide a strong consistency check on inflation.

The potential power of the microwave background is demonstrated by the fact that inflation, a theoretical mechanism which likely would occur at energy scales not too different from the Planck scale, would result in several distinctive signatures in the microwave background radiation. Current measurements beautifully confirm a flat universe and are fully

consistent with gaussian perturbations; the rest of the tests will come into clearer view over the coming years. If inflation actually occurred, we can expect to have very strong circumstantial supporting evidence from the above signatures, along with precision measurements of the cosmological parameters describing our universe. On the other hand, if inflation did not occur, the universe will likely look different in some respects from the space of models in Sec. 6.1. In this case, we may not be able to recover cosmological parameters as precisely, but the microwave background will be equally important in discovering the correct model of our universe.

I thank the organizers for a stimulating and enjoyable Summer School. The preparation of these lectures has been supported by the NASA Astrophysics Theory Program and the Cotrell Scholars program of the Research Corporation.

## REFERENCES

- Adams W S 1941 *Astrophys. J.* **93** 11
- Albrecht A 2000 to appear in *Structure Formation in the Universe* ed. Crittenden R and Turok N (Kluwer) astro-ph/0007247
- Alpher R A and Herman R C 1949 *Phys. Rev.* **75** 1089
- Bardeen J M 1980. *Phys. Rev. D* **22** 1882
- Bennett C L *et al.* 1994 *it Astrophys. J.* **464** L1
- Birkinshaw M 1999 *Phys. Rep.* **310** 97
- Bond J R, Efstathiou G, and Tegmark M 1997 *Mon. Not. R. Ast. Soc.* **291** L33
- Bouchet F R and Gispert R 1999 *New Astron.* **4** 443
- Bucher M, Moodley K, and Turok N 1999 *Phys. Rev. D* **62** 083508
- Caldwell R R, Dave R, and Steinhardt P J 1998 *Phys. Rev. Lett.* **80** 1582
- Challinor A and Lasenby A 1999 *Astrophys. J.* **513** 1
- Christensen N and Meyer R 2000 astro-ph/0006401
- Cornish N J, Spergel D N, and Starkman G D 1998 *Phys. Rev. D* **57** 5982

- de Bernardis P *et al.* 2000 *Nature* **404** 955
- Denisse J F, Le Roux E, and Steinberg J C 1957 *Comptes Rendus de l'Academie des Sciences* **244** 3030 (in French)
- Dicke R H, Peebles P J E, Roll P G, and Wilkinson D T 1965 *Astrophys. J.* **142** 414
- Dodelson S, Gates E, and Stebbins A 1996 *Astrophys. J.* **467** 10
- Doroshkevich A G and Novikov I D 1964 *Sov. Phys. Dokl.* **9** 111
- Ehlers J 1993 *Gen. Rel. Grav.* **25** 1225
- Ellis G F R and Bruni 1989 *Phys. Rev. D* **40** 1804
- Esposito S, Mangano G, Miele G, and Pisanti O 2000 *J. High En. Phys.* **9** 038
- Falco E E, Kochanek C S, and Munoz J A 1998 *Astrophys. J.* **494** 47
- Ferreira P G, Magueijo J, and Silk J 1997 *Phys. Rev. D* **56** 4592
- Gamow G 1956 *Vistas in Astron.* **2** 1726
- Gebbie T, Dunsby P, and Ellis G F R 2000 *Ann. Phys.* **282** 321
- Gnedin N Y and Jaffe A H 2000 astro-ph/0008469
- Hamilton A J and Tegmark M. 2000 preprint astro-ph/0008392
- Hanany S *et al.* 2000 *Astrophys. J.* in press
- Harari D D, Hayward J, and Zaldarriaga M 1996 *Phys. Rev. D* **55** 1841
- Hu W 2000 *Astrophys. J.* **529** 12
- Hu W and Gruzinov A 1998 *Astrophys. J.* **508** 435
- Hu W and Silk J 1993 *Phys. Rev. Lett.* **70** 2661
- Hu W and Sugiyama N 1996 *Astrophys. J.* **471** 542
- Hu W and White M 1996 *Astrophys. J.* **471** 30
- Hu W and White M 1997 *Astron. Astrophys.* **321** 8
- Hu W, Seljak U, White M and Zaldarriaga M 1998 **57** 3290

- Huterer D and Turner M S 2000 *Phys. Rev. D* **62** 063503
- Jackson J D 1975 *Classical Electrodynamics* 2nd ed. (New York: Wiley)
- Jaffe A H and Kamionkowski M 1998 *Phys. Rev. D* **58** 043001
- Jaffe A H, Stebbins A, Frieman J A 1994 *Astrophys. J.* **420** 9
- Jungman G, Kamionkowski M, Kosowsky A, and Spergel D N 1996 *Phys. Rev. D* **54** 1332
- Kahniashvili T, Mack A, Kosowsky A, Durrer R 2000 to appear in *Cosmology and Particle Physics 2000*, ed. Garcia-Bellido J, Durrer R, and Shaposhnikov M
- Kamionkowski M and Kosowsky A 1998 *Phys. Rev. D* **67** 685
- Kamionkowski M and Kosowsky A 1999 *Ann. Rev. Nucl. Part. Sci.* **49** 77
- Kamionkowski M, Kosowsky A, and Stebbins A 1997a *Phys. Rev. Lett.* **78** 2058
- Kamionkowski M, Kosowsky A, and Stebbins A 1997b *Phys. Rev. D* **55** 7368
- Kamionkowski M, Spergel D N, and Sugiyama N 1994 *Astrophys. J. Lett.* **426** L57
- Kaplinghat M and Turner M S 2000 *Phys. Rev. Lett.* in press
- Knox L 1995 *Phys. Rev. D* **52** 4307
- Knox L, Scoccimaro R, and Dodelson S 1998 *Phys. Rev. Lett.* **81** 2004
- Kodama H and Sasaki M 1984 *Prog. Theor. Phys. Suppl.* **78** 1
- Kolb E W and Turner M S 1990 *The Early Universe* (Redwood City: Addison Wesley)
- Kosowsky A 1996 *Ann. Phys.* **246** 49
- Kosowsky A 1999 *New Astron. Rev.* **43** 157
- Kosowsky A and Loeb A 1996 *Astrophys. J.* **469** 1
- Kosowsky A and Turner M S 1995 *Phys. Rev. D* **52** 1739
- Kragh, H 1996 *Cosmology and Controversy* (Princeton: Princeton University Press)
- Lange A *et al.* 2000 astro-ph/0005004
- Lidsey J E *et al.* 1997 *Rev. Mod. Phys.* **69** 373

- Ma C P and Bertschinger E 1995 *Astrophys. J.* **455** 7
- McKellar A 1940 *Proc. Ast. Soc. Pac.* **52** 187
- Miller A *et al.* 1999 *Astrophys. J.* **524** L1
- Mould J, Kennicutt R C, and Freedman W 2000 *Rep. Prog. Phys.* **63** 763
- Mukhanov V F, Feldman H A, and Brandenberger R H 1992 *Phys. Rep.* **215** 203
- Mukhanov V F and Steinhardt P J 1998 *Phys. Lett.* **B422** 52
- Peacock J A *et al.* 1998 *Mon. Not. R. Ast. Soc.* **296** 1089
- Penzias A A and Wilson R W 1965 *Astrophys. J.* **142** 419
- Perlmutter S *et al.* 1999 *Astrophys. J.* **517** 565
- Polarski D and Starobinsky A A 1994 *Phys. Rev. D* **50** 6123
- Riess A G *et al.* 1998 *Astron. J.* **116** 1009
- Sachs R K and Wolfe A M 1967 *Astrophys. J.* **147** 73
- Seager S, Sasselov D, and Scott D 2000 *Astrophys. J. Suppl.* **128** 407
- Seljak U 1996 *Astrophys. J.* **463** 1
- Seljak U, Pen U, and Turok N 1997 *Phys. Rev. Lett.* **79** 1615
- Seljak U and Zaldarriaga M 1996 *Astrophys. J.* **469** 437
- Sellwood J and Kosowsky A 2000 to appear in *Gas and Galaxy Evolution* eds. Hibbard J E, Rupen M P, and van Gorkom J, in press
- Sharov A S and Novikov I D 1993 *Edwin Hubble, the Discoverer of the Big Bang Universe* (Cambridge: Cambridge University Press)
- Smoot G F *et al.* 1990 *Astrophys. J.* **360** 685
- Tegmark M, Zaldarriaga M, and Hamilton A J S 2000 astro-ph/0008167
- Tegmark M and Zaldarriaga M 2000 *Astrophys. J.* in press
- Thorne K S 1980 *Rev. Mod. Phys.* **52** 299

- Tolman R C 1934 *Relativity, Thermodynamics, and Cosmology* (Oxford: Oxford University Press)
- Tytler D et al 2000 *Phys. Scripta* in press, astro-ph/0001318
- Weeks J R 1998 *Class. Quant. Grav.* **15** 2599
- Weinberg S 2000 preprint astro-ph/0005265
- White M, Scott D, and Silk J 1994 *Ann. Rev. Astron. Astrophys.* **32** 319
- Zaldarriaga 1997 *Phys. Rev. D* **55** 1822
- Zaldarriaga M and Seljak U 1997 *Phys. Rev. D* **55** 1830
- Zaldarriaga M, Seljak U, and Spergel D N 1997 *Astrophys. J.* **488** 1
- Zaldarriaga M and Spergel D N 1997 *Phys. Rev. Lett.* **79** 2180